NATIONAL ADVISORY COMMITTEE FOR AERONAUTICS

WARTIME REPORT

ORIGINALLY ISSUED
September 1943 as
Advance Restricted Report 3I06

SOME ANALYSES OF SYSTEMATIC EXPERIMENTS ON THE RESISTANCE AND PORPOISING CHARACTERISTICS OF FLYING-BOAT HULLS

By Kenneth S. M. Davidson and F. W. S. Locke, Jr.
Stevens Institute of Technology

NACA

WASHINGTON

NATIONAL ADVISORY COMMITTEE FOR AERONAUTICS

ADVANCE RESTRICTED REPORT

SOME ANALYSES OF SYSTEMATIC EXPERIMENTS ON THE RESISTANCE AND PORPOISING CHARACTERISTICS OF FLYING-BOAT HULLS

By Kenneth S. M. Davidson and F. W. S. Locke, Jr.

SUMMARY

This report discusses certain analyses and condensations of the test results obtained in the extensive series of systematic experiments on the porpoising charteristics of flying boats reported in reference 1. The work is believed to simplify application of the test results to practical design problems and to aid in clarifying basic concepts regarding porpoising.

The experiments were carried out according to strict system and considerable attention was given, in reference 1, to presenting the results in a form which would provide as clear a visual impression as possible of the influence and relative importance of the different variables. The radiating chart of variables in figure 1 and the condensed summary charts of test results in figures 2 and 3 are taken from reference 1 and furnish the general background for the analyses here considered.

It is concluded in this report that:

I - For a given hull form under various combinations of loading and aerodynamic conditions

(a) The stability limits are determined

(1) Primarily by the net water-borne load in steady motion Δ

(2) Secondarily by the tail damping rate M_q (sec. 3)

This means a reduction in the number of variables which have to be considered from the total of twelve covered by the experiments

(in groups I and II) to only two. The separate effects of gross load Δ_o, wing lift at arbitrary trim angle Z_o, and rate of change of lift with trim Z_θ are concentrated into the all-inclusive variable net water-borne load Δ; the tailing damping rate M_q is the only other controlling variable.

(b) The curves of stability limits are satisfactorily expressed as

(1) Functions of the dimensionless criterion $\sqrt{C_\Delta}/C_V$, which relates net water-borne load with speed

(2) With the dimensionless criterion for tail damping $\dfrac{M_q}{V\frac{\rho_w}{2}b^4}$ (where ρ_w is water density), as a parameter (secs. 4 and 5, chart in fig. 6).

One advantage of expressing the limits in this manner is that the porpoising characteristics of the hulls of different flying boats can be compared directly, without regard to differences in the aerodynamic structures. Another, and perhaps more important, advantage is that the stability data are readily available for use in the preliminary design stage, to deduce the hydrodynamic performance of proposed ships with various aerodynamic structures, or even before the aerodynamic structure has been considered in detail.

II – <u>For modifications of the afterbody derived from the same parent, under given loading and aerodynamic conditions</u>

(a) The upper stability limit and the peak of the lower stability limit (at moderate speeds) are raised or lowered if the modification raises or lowers the stern-post angle, and in substantially equal amount (sec. 10, chart in fig. 10).

(b) The lower limit at high speeds is not affected (chart in fig. 9).

(c) The hump trim follows the changes in stern-post angle in the same way as the limit curves in (a), and the hump resistance is primarily a function of the hump trim (sec. 14, chart in fig. 15).

(d) The effectiveness of the ventilation of the main step determines the presence or absence of upper-limit porpoising at high speeds, more effective ventilation suppressing this type of porpoising (sec. 13).

These conclusions are based upon a consideration of those variables on the radiating chart on figure 1 which are not covered by cross-hatching. The remaining variables have not yet been considered, and the cross-hatching has been added to the chart to make this clear. It is believed that the remaining variables can be treated in a generally similar way to those considered at this time, but the work to date is being presented without waiting for further analyses because it seems of sufficient interest in itself.

By considering the analyses so far completed and by some extent anticipating future analyses of variables not yet completed, it seems clear that when the stability limits are expressed as functions of $\sqrt{C_\Delta}/C_V$ with $\frac{M_q}{V \frac{\rho_w}{2} b^4}$ constant.

(1) The positions of the upper stability limit and of the peak of the lower stability limit are governed primarily by

(a) The stern-post angle (the angle between a tangent to the forebody keel at the step and a line joining the tip of the step with the tip of the stern post)

(b) The power (i.e., dynamic lift) of the second step (as influenced by the plan area in the vicinity of the stern post, the general angle

of attack of this area with respect to the line joining the tip of the stern post with the tip of the main step, chine flare, etc.)

(2) The position of the lower stability limit at high speeds is governed primarily by

(a) The dead rise and the effective warping of the forebody bottom, and probably also the curvature of the forebody buttocks

(3) Suppression of upper-limit porpoising at high speeds is governed primarily by

(a) The effectiveness of the ventilation of the afterbody bottom in the vicinity of the main step

Of the foregoing, 1(b) and 2(a), while based on the test data reported in reference 1, are not analyzed in this report.

These broad conclusions constitute a powerful tool for clarifying porpoising phenomena, even though they may not be found strictly applicable, in their entirety, to all cases. The main concepts are brought out rapidly in the following diagram:

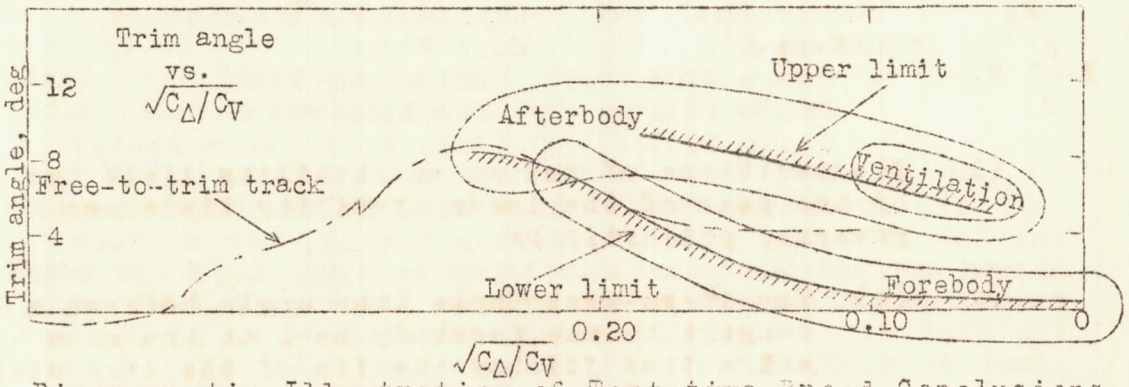

Diagrammatic Illustration of Tentative Broad Conclusions regarding Porpoising
showing
the stability limits in nondimensional form
and the regions influenced
by the forebody
by the afterbody
by ventilation

In this figure, the closed curve surrounding the lower limit indicates the area within which changes to the forebody are effective in altering the position of the lower limit of stability. Similarly, the closed curve surrounding the upper limit and peak of the lower limit indicates the area in which changes to the afterbody are effective. Likewise, the line around the right-hand end of the upper limit indicates the area within which step ventilation is effective.

INTRODUCTION

The systematic experiments considered in reference 1 radiated from a given flying boat taken as a basic point of departure. Each of a number of variables was altered, separately from the others, over a range of values embracing the normal value for the flying boat and intended to be wide enough to cover all values likely to be encountered in practice. The advantage of this procedure is that it materially simplifies the problem of coordinating test results. It enables the effect to be estimated of making corresponding changes in designs other than that of the reference flying boat in the majority of cases.

The variables fall naturally into the following groups:

Group I	Weight and Inertia Loading
Group II	Aerodynamic Conditions
Group III	Hull Form
Group IIIA	Afterbody Form
Group IIIF	Forebody Form
Group IIIH	Hull Form (as a whole)

The reference flying boat used in the experiments was the XPB2M-1, a modern design having, for a gross weight of 140,000 pounds, a wing loading Δ_o/S of 38.0 pounds per square foot and a beam loading Δ_o/wb^3 of 0.89. The dimensions and particulars considered as normal are given in table I.

The present discussions consider the variables of groups I and II and some of the variables of group IIIA. All conclusions and generalizations are based upon the ranges of change of the variables covered in the experiments. Had the changes been extended ad absurdum, some of the conclusions would undoubtedly have been altered.

This investigation, conducted at the Stevens Institute of Technology, was sponsored by, and conducted with financial assistance from the National Advisory Committee for Aeronautics.

DISCUSSION

Group I — Weight and Inertia Loading

Group II — Aerodynamic Conditions

1. These two groups include all of the variables responsible for forces or moments acting on the hull other than hydrodynamic.

The variables of group I are obvious at once; those of group II are scarcely less obvious, thanks to the relatively simple configuration of the airplane. Thus it can be said with some assurance that the list given on the radiating chart in figure 1 includes all of the variables in these two groups which affect forces and moments applied to the hull, both in steady motion and in porpoising.

The mass in vertical oscillation is an additional variable which, like the aerodynamic component of Z_w and one or two other of the aerodynamic derivatives, can be made independent (in this case, independent of gross weight) in the model but not in the ship. Though not considered directly in the experiments, it was considered indirectly as explained in the next section.

The symbols on the radiating chart indicate the variables in these groups which are found to have:

Three open circles — no effect on steady-motion resistance, as determined by inspection

Three blacked circles — very little or no effect on the stability limits as shown by the experiments. (See figs. 2 and 3.)

It will be seen that, of the twelve variables necessarily considered at the start, six can be ruled out immediately as having no important effect on either resistance or porpoising.

2. Regarding the six remaining variables, it is apparent that

(1) Δ_o, Z_o, and Z_θ, in combination, fix a net force which is, in fact, the net water-borne load in steady motion Δ

(2) The center of gravity position and M_o, in combination, fix a net moment which determines the trim angle in steady motion τ

(3) M_q determines, by itself, the tail damping moments in porpoising motion

These combinations strongly suggest that, instead of six, the controlling variables are really three; namely,

(1) Net water-borne load Δ affecting resistance and porpoising

(2) Net moment M affecting resistance and porpoising

(3) Tail damping rate M_q affecting porpoising only, not resistance

Now it is known to begin with, of course, that the steady-motion resistance is controlled by the first two of these as indicated and that M_q affects porpoising. Evidence that, with M_q fixed, the first two control porpoising is supplied

(1) By the upper charts (a) in figure 4, where it is seen that the upper and lower porpoising limits obtained in the separate experiments for altered values of Δ_o, Z_o, and Z_θ, respectively, can be expressed as unique functions of the net water-borne load Δ, with discrepancies of less than 1^o.

It may be noted here, though it bears mainly on the discussion of the preceding section, that when Δ is altered by changing Δ_o the mass in vertical oscillation is affected in direct proportion but that when Δ is altered by changing Z_o or Z_θ the mass is unaffected. Hence, a demonstration that Δ is the controlling variable, whether the mass is varied or not, is in effect a demonstration that the mass in vertical oscillation does not affect porpoising.

(2) By the more comprehensive charts of the same sort in figures 5 and 6 discussed in section 4.

The lower charts (b) in figure 4 show that the shifts in the moment curves obtained in the separate experiments for altered center-of-gravity locations correspond to the product of the center-of-gravity shift times the net water load, as would be expected; thus the net moment M is the controlling variable.

3. In practice, resistance is usually given as a function of trim, load, and speed, and porpoising limits are frequently expressed in terms of trim and speed - in both cases without special regard to the availability of the moments required to produce the stated trims. In other words, moment is not ordinarily treated as an independent variable, trim being substituted arbitrarily as a parameter. This substitution of trim for moment is discussed in more detail in the appendix. By making the substitution, and by restating the concepts of the preceding section, it may be said that

(1) The resistance characteristics are a function of trim, load, and speed.

(2) The porpoising characteristics are primarily functions of load and speed, and secondarily functions of the tail-damping rate.

The controlling variables are then reduced to two. Furthermore, the tail-damping rate affects primarily the lower porpoising limit at high speeds (see fig. 2) and is clearly of less importance than the net water-borne load.

4. A further simplification in the statement of the porpoising characteristics is effected when the stability limits are plotted against Δ/V^2, instead of Δ and speed is thereby eliminated as a separate consideration. This is shown in the chart in figure 5, which includes the data from the upper charts (a) in figure 4 and additional data for other speeds. Two scales of abscissas are given Δ/V^2 and the corresponding nondimensional criterion $C_\Delta/C_V{}^2$ [$\frac{1}{2}$(lift coefficient, $\Delta/b^2\,\rho_w/2\,V^2$)].

An alternate, and somewhat preferable, form of plotting for this chart is shown in figure 6. Here the abscissas are $\sqrt{C_\Delta}/C_V$ instead of $C_\Delta/C_V{}^2$ and the scale is reversed.

In this form the curves look more familiar and they are less distorted.

The same simplification has been applied in the past with reasonable success to resistance data for the planing range (see references 2 and 3); its success for porpoising data is not, therefore, very surprising. Nor need the fact that it has never been widely used in dealing with resistance data necessarily influence its adoption for porpoising data; the high precision required for resistance information is not ordinarily needed for stability limits. Its use reduces the statement of porpoising characteristics to a single chart with M_q as a parameter.

The extent of the speed ranges over which porpoising occurs under various conditions, and particularly the presence or absence of upper-limit porpoising at high speeds, are not indicated by such charts. These are discussed in section 13.

5. The tail-damping derivative M_q is directly proportional to speed. Hence, a statement of the proportionality factor M_q/V is sufficient to define values for all speeds. When divided by $\rho_w/2\ b^4$ (ρ_w for water), this factor is made nondimensional; the expression $\dfrac{M_q}{V \frac{\rho_w}{2} b^4}$ is therefore a suitable criterion with which to express the tail-damping rates for a given design, at all speeds and sizes. Its value is 0.249 for the experiments in question.

6. In summation it appears that the porpoising characteristics of a given hull can be expressed (with the reservation noted at the end of sec. 4) by a single chart with a single parameter. The inherent porpoising characteristics, which fix the shapes and positions of the limit curves on this chart for a given value of the parameter, must then depend on hull form only.

Group III

Hull Form

7. The choice of variables for systematic studies of hull form is by no means straightforward. The hydrodynamic com-

ponents of such quantities as Z_θ, M_q, and so forth, are not clearly related to geometric configurations and sizes of specific elements of the hull form in the simple fashion that the aerodynamic components are clearly related to geometric configurations and sizes of specific elements of the airplane. Hull form must therefore be dealt with as such.

The ends sought are easily stated:

(a) To reduce hump and high-speed resistance

(b) To eliminate porpoising or, failing this, to widen the range of stable trim angles

It is desirable to improve both characteristics, and improvement of one at the expense of the other will not usually be very helpful.

It will be understood that with any hull form it is necessary to locate the center of gravity so that the hump resistance is reasonable, and so that the available trim tracks are within the stability limits at planing speeds.

8. In the experiments (reference 1) the choice of variables was governed by the underlying concept that the forebody and afterbody are separate parts of the hull serving different purposes and that in consequence each should be altered independently of the other.

This concept was suggested by the comparison shown in figure 7, between the characteristics of the complete hull and those of the forebody alone (under otherwise identical conditions). This comparison was worked out before the list of hull modifications was decided upon; as explained in reference 1, it reveals in particular

(a) That the afterbody is useful only in the lower half of the speed range to take-off and that its presence at higher speeds is entirely detrimental; that

At rest and at displacement speeds, it provides flotation

At moderate speeds up to the hump, it controls trim and resistance and prevents lower-limit porpoising

At high (planing) speeds, it is the direct cause of upper-limit porpoising and somewhat increased resistances

(b) That the forebody is entirely self-sufficient at planing speeds and needs no help from the afterbody

These indications suggest clearly

(a) That the forebody is the main hull - essentially a stepless, V-bottom, planing boat with the center of gravity very far aft

(b) That the afterbody is an appendage, the function of which is to control trim (by providing nosing-down moment) until true planing of the main hull is established

Group III is accordingly divided into three subgroups

Group IIIA	Afterbody Form
Group IIIF	Forebody Form
Group IIIH	Hull Form (as a whole)

The first two of these are of more interest for present purposes than the third and, as explained previously, only a part of the first is dealt with in this report.

Group IIIA

Afterbody Form

9. When a given set of vertical transverse sections (that is, a given body plan) is used to produce a series of hull forms differing in some consistent fashion in their proportions, the resulting forms are said to spring from the same parent form. It is only when, regardless of proportions, the shape of one or more sections is altered with respect to the others that the parent form is said to have been altered.

It is in accordance with these ideas to refer to the following variables of group IIIA as involving no changes of parent form:

Afterbody angle Step height	for changing which, the same afterbody was used in the experiments
Afterbody length	for changing which, the afterbody station spacing was uniformly altered

The present discussion is limited to these variables with some reference to the experiments with the forebody alone.

10. Figure 8 shows the porpoising limits for the above-mentioned variables. The lower-limit curve for the forebody alone is added to these charts for reference.

Figure 9 shows the same limits replotted against $\sqrt{C_\Delta}/Cv$ reversed (after the manner of fig. 6).

Figure 10 shows a second replotting, in which the reversed scale of $\sqrt{C_\Delta}/Cv$ is retained for the abscissas but the limits are referred to absolute stern-post trim instead of forebody trim. By arbitrary definition, (absolute stern-post trim) = (absolute forebody trim) - (stern-post angle). This definition is illustrated by a sketch on the chart.

Referring to the three charts (figs. 8 to 10) it will be seen that

(1) The lower limit at high speeds is not affected by alterations to any of the three variables considered. This might be expected from the fact that even so extreme a change as removing the afterbody entirely (see fig. 7) had practically no effect.

(2) The "break-away" of the lower-limit curve from the basic curve for the forebody alone and the position of the upper-limit curve are functions of the stern-post angle primarily.

With respect to the second of these generalizations, figure 10 shows in particular that

The peaks of the break-aways of the lower-limit curves can be reasonably well represented by an envelope curve, which isolates the effect of the afterbody on lower-limit porpoising

The individual points for the upper-limit do not scatter more from the mean curve than the points in figure 6, the mean curves on these two charts being consistent with each other.

Figure 10 may be regarded as providing a further simplification (following fig. 6) in the statement of porpoising characteristics. By eliminating differences directly attributable to differences of stern-post angle, it clarifies one more variable in the analysis of porpoising characteristics. Like figure 4, however, it fails to take into account differences in the ranges of speed (or of $\sqrt{C_\Delta}/C_V$) over which upper-limit porpoising occurs under various conditions. It fixes the position of the upper-limit curve but not the extent. The latter is considered further in section 13.

11. It is clear from the discussion of the preceding section that the limit curves in figure 10 are substantially independent of the forebody trim. It is seen, too, that the total range of stern-post trims embraced by the two limit curves is quite small (of the order of 4°). These observations suggest strongly that the wake, or trough, left by the forebody must be substantially independent of the forebody trim and relatively flat at all planing speeds.

12. The photographs (figs. 11 to 13) were taken in an attempt to throw further light on the nature of the flow patterns in the vicinity of the porpoising limits. Three regions are shown, in separate figures:

Lower limit at peak of break-away (fig. 11)
Upper limit at moderate planing speeds (fig. 12)
Upper limit at high planing speeds (fig. 13)

Each region is illustrated by three cases:

Afterbody angle, 12°
Afterbody angle, 7°
Afterbody angle, 4½°

and each case has three photographs for trim angles covering a range of 2° in the vicinity of the porpoising limit under consideration.

These photographs should be viewed as a first attempt to illustrate the flow patterns. They indicate, however,

(1) Regarding lower-limit porpoising (fig. 11) - that this type of porpoising is suppressed when, with increasing trim angle, the tip of the afterbody first makes contact with the water surface (this indication being amply confirmed by visual observations of the model during tests). Since this occurs with stern-post depressions of the order of 1° to 3°, it is evident that the forebody wake is depressed in about the same amount at the values of $\sqrt{C_\Delta}/C_V$ in question.

(2) Regarding upper-limit porpoising (figs. 12 and 13) - that this type of porpoising develops when, with an increase of trim of the order of 1° to 2° beyond that required to suppress lower-limit porpoising, a large portion of the afterbody bottom becomes wetted. This wetting and the fact that it is followed, when the trim is further increased by about 1°, by the forebody coming clear, so that only the tip of the afterbody remains in contact with the water surface, seems to go far toward explaining the mechanism of upper-limit porpoising. Evidently the wetting of the afterbody introduces forces (and moments) which result in the forebody jumping clear and this in turn breaks up the situation which caused the afterbody wetting.

The photographs in figure 14 were taken to illustrate the similarity of the flow patterns at fixed values of $\sqrt{C_\Delta}/C_V$ obtained with different combinations of C_Δ and C_V. As such, they properly belong with the discussion of section 4 rather than here. They are of interest in connection with the present discussion, however, because they indicate that $\sqrt{C_\Delta}/C_V$ is a very exact criterion of flow similarity when other things are equal, and they therefore provide a background for saying that very small differences observed in the other photographs - where other things are not equal - may be significant.

13. It has been noted, in sections 4 and 10, that the extent of the speed range over which upper-limit porpoising occurs is not necessarily shown in condensations of test data upon the base $\sqrt{C_\Delta}/C_V$. This speed range or, more

especially, the range of high speeds over which upper-limit porpoising is absent, has considerable practical importance. The absence of upper-limit porpoising is obviously desirable in itself, and there is a possibility (now under investigation) that its presence or absence is associated with undesirable or desirable, respectively, landing characteristics.

Reference to figures 8 and 9 indicates:

(1) That, if the upper-limit curve stops short of take-off, it tends to stop at more nearly a constant value of $\sqrt{C_\Delta}/Cv$ (roughly 0.09) than a constant value of speed

(2) That the upper-limit curve stops short of take-off when

(a) The stern-post angle is increased above the normal value of 8°

(b) The step height is increased above the normal value of 5 percent of the beam

(c) In spite of a very low step height (1 percent), a substantial passage is provided to allow air to reach the rear of the step

Now it will be seen that, in all three of the cases listed under (2), there has been an increase in the amount of step ventilation, this term being used broadly, to include any means by which a supply of air to the step can be accomplished and not merely the provision of air ducts. The inference is obvious that the avoidance of high-speed upper-limit porpoising depends directly on the provision of sufficient ventilation. This inference, furthermore, appears to be entirely consistent with the point of view developed in section 12 that the wetting of a large portion of the afterbody bottom marks the beginning of upper-limit porpoising, for general wetting of the afterbody bottom is probably associated closely with the effectiveness of step ventilation.

14. Figure 15 is a chart of maximum hump resistance plotted against maximum hump trim. Values are for the true hump (in the vicinity of 10 ft/sec model speed) and not for the ventilation hump (in the vicinity of 8 ft/sec). Data are included for one or two

variables in addition to those listed in section 9 in order to emphasize that it is the hump trim itself, rather than the exact means taken to get it, which controls the hump resistance. The excess of the total resistance over the value of $\Delta \tan(\tau+2^{\circ})$ is seen to be roughly constant for high trims but to increase rapidly with low trims so that the total resistance is a minimum at around $3\frac{1}{2}^{\circ}$ trim.

The arrows on the chart indicate the difference between the maximum hump trim and the maximum trim on the curve of lower-limit porpoising (which usually occurs at much the same speed). The hump trim exceeds the lower porpoising limit to a moderate extent except when the hump trim is very low.

CONCLUSIONS

The principal conclusions to be drawn have already been stated in the Summary of the report.

Particular attention is called to the three charts:

Figure 6 — which shows that, for a given hull under various combinations of loading and aerodynamic conditions, the stability limits may be expressed as functions of the dimensionless criterion $\sqrt{C_{\Delta}}/C_V$ with $\frac{Mq}{V\frac{\rho_w}{2}b^4}$ as a parameter.

Figure 10 — which shows that, for modifications of the afterbody derived from the same parent, under given loading and aerodynamic conditions, the upper stability limit and the peak of the lower stability limit are raised or lowered as the stern-post angle is raised or lowered, and in like amount.

Figure 15 — which shows that the hump resistance is a direct function of the hump trim, the latter in turn following changes of the stern-post angle.

Experimental Towing Tank,
Stevens Institute of Technology,
Hoboken, N. J., July 10, 1943.

APPENDIX

While not strictly a part of the present thesis, a brief discussion of the substitution of trim for moment as a criterion in the statements of resistance and porpoising characteristics may be useful.

Moment is, in fact, an independent variable and failure to consider it as such does not dispose of it. There can be little advantage in knowing best trims (with respect to either resistance or porpoising) without knowing whether they can be obtained. The general lack of emphasis on moment is perhaps explained in part by the difficulties which still stand in the way of accurate determinations of the aerodynamic moments during take-off and landing. There is another aspect of the matter, however, which is considered in what follows.

The chart in figure 16 shows the usual data for the normal XPB2M-1 flying boat and, at the four speeds for which cross plots are drawn, the moments due to

(1) Thrust —
Corresponding to the thrust curve shown.

(2) Maximum shift of center of gravity —
Corresponding to $2\frac{1}{2}$ feet either way in the ship or 18.5 percent of the beam. (The wing is assumed to be shifted with the c.g.)

(3) Maximum elevator deflection —
Assuming $C_{M_{max\ aero}} = 0.4$ (or $C_{L_t} = 1.0$)

These are the principal moments; they are additive (algebraically), except for the thrust moment, in any desired combination. The magnitudes shown are not claimed to have precise absolute significance; they are intended only to indicate approximate maximums. With this understanding, it will be observed that

(1) At the lowest speed ($C_V = 2.79$), which is about at the hump and for which the power-on case is therefore of most interest, the possible effect on trim of altering the moment combination is about $2\frac{1}{2}^0$ and that
Any trim within this range is near the trim for best resistance,

(2) At the highest speed (C_V = 5.57) the elevator moment is so large that, with any combination of the other two moments, the trim can be held between the porpoising limits and at the value for best resistance

For these two speeds, then (and for all lower and higher speeds, respectively) moment is of secondary interest only. However,

(3) At the first intermediate speed (C_V = 3.71), the trim for least resistance can be reached with any possible combination of the moments, but this trim is less than the lower porpoising limit, and there are many combinations of the moments, particularly in the power-on case, with which the maximum trim cannot be made to exceed the lower limit.

Thus, for speeds in the vicinity of this one (a little above the hump) moment, though still secondary from the point of view of steady-motion resistance, takes on primary importance from the point of view of porpoising limits. These speeds, too, are especially important because in accelerated take-off the trim is falling rapidly from its peak value near the hump; thus initial disturbances are provided to help induce porpoising.

In general, therefore, moment has to be given more consideration in dealing with porpoising than in dealing with resistance. But there does not seem to be any great need for a more accurate knowledge of the aerodynamic (elevator) moment; the principal requirement is to get the center of gravity in the most advantageous position.

Shifting the center-of-gravity position is much the simplest way to alter the moment combination in an existing flying boat, and tests to determine the best position - or the limiting practicable range of positons - are ordinarily carried out on a new flying boat. In this case, however, the consequences of a shift differ somewhat from those discussed in section 2 because the wing is not shifted with the center of gravity. From the point of view of design, with which this paper is primarily concerned, the wing ought usually to be shifted when the center of gravity is shifted to avoid introducing an additional moment while flying. This was

simulated in the experiments which form the background for the present work and allowed for in calculating the moments for the charts in figure 16. When the wing is not shifted, the moment is greater, as indicated in the following sketches:

Wing shifted
Change moment = $(\Delta_o - L)$ a

Wing not shifted
Change moment = Δ_o a

The difference is mentioned here to avoid possible misunderstanding.

REFERENCES

1. Davidson, Kenneth S. M., and Locke, F. W. S., Jr.: Some Systematic Model Experiments on the Porpoising Characteristics of Flying-Boat Hulls. NACA A.R.R., June 1945.

2. Schröder, Paul: The Take-Off of Seaplanes, Based on a New Hydrodynamic Reduction Theory. T.M. No. 621, NACA, 1931.

3. Anon.: A Comparison of Stevens and N.A.C.A. Tests in the Planing Range of the Navy Mark V Seaplane Hull. T.M. No. 47, Stevens Inst. Tech., 1940.

TABLE I

DIMENSIONS AND PARTICULARS (NORMAL) FOR FULL-SIZE FLYING BOAT XPB2M-1 AND $\frac{1}{30}$-SCALE MODEL

Dimensions	Full size	1/30-scale model
Beam at main step, in	162	5.40
[a]Angle between forebody keel and base line, deg	2.0	2.0
Angle between afterbody keel and base line, deg	5.0	5.0
Height of main step at keel, in	8.1	0.27
Center of gravity forward of main step (26.58 percent M.A.C.), in	70	2.33
Center of gravity above base line, in	146.7	4.89
Gross weight, Δ, lb	140,000	5.19 f.w.
Load coefficient, C_Δ (sea water)	0.89	
Moment of inertia in pitch, slug-ft^2	1.366×10^6	
lb-in^2	6.328×10^9	260
Wing span, ft	200	6.67
Wing area, S, sq ft	3683	4.092
Mean aerodynamic chord, M.A.C., in	249	8.30
Aspect ratio (geometric)	10.87	10.87
Horizontal tail area, sq ft	508	0.565
Elevator area, sq ft	143.7	0.160
Distance c.g. to 35 percent M.A.C. horizontal tail (tail length), ft	63.6	2.12
Thrust line above base line at main step, in	230.3	7.68
Thrust line inclined upward to base line, deg	5.5	5.5

Ratios $\frac{\text{Full-size}}{\text{Model}}$,

Of velocities, $\lambda^{1/2}$	5.477
Of linear dimensions, λ	3.0×10
Of areas, λ^2	9.0×10^2
Of volumes, λ^3	27.0×10^3
Of moments, λ^4	81.0×10^4
Of moments of inertia, λ^5	243.0×10^5

[a]See footnote on p. 21.

TABLE I

DIMENSIONS AND PARTICULARS (NORMAL) FOR FULL-SIZE FLYING BOAT XPB2M-1 AND $\frac{1}{30}$-SCALE MODEL (Continued)

Aerodynamic characteristics	Full size	1/30-scale model
C_L at $\tau = 5^\circ$ (relative to base line, flaps, 30°)	1.585	1.585
L at $\tau = 5^\circ$	$6.95\ v_{s(c)}^2$	$7.72 \times 10^{-3}\ v^2$
$dC_L/d\tau$	0.1045	0.1045
$dL/d\tau$ $(dZ/d\theta)$, lb/deg	$0.458\ v_s^2$	$0.509 \times 10^{-3}\ v^2$
dL/dw (dZ/dw), lb-sec/ft $\left(\frac{dL}{d\tau}\frac{1}{v}\right)$	$0.458\ v_s$	$0.509 \times 10^{-3}\ v$
$dC_{M_{CG}}/d\alpha_{BL} = dC_{M_{CG}}/d\tau$ (av.)	0.0150	0.0150
$dM_{CG}/d\tau$ $(dM/d\theta)$, lb ft/deg (av.)	$1.365\ v_s^2$	$5.05 \times 10^{-5}\ v^2$
[b] dM/dq, lb ft sec/radian	$8020 \times v_s$	$9.90 \times 10^{-3}\ v$
dM/dw, lb sec (av.)	$78.3 \times v_s$	$2.90 \times 10^{-3}\ v$
$\frac{dM/dq}{dM/dw}$, ft/radian	102.5	3.41
$\frac{dM/dq}{dM/dw}$ /Tail length, 1/radian	1.61	1.61
Get-away speed, fps	130	23.74
Get-away C_L	1.890	1.890
Get-away τ, deg	8.8	8.8

[a] All trim angles measured relative to the base line.
[b] Contribution of horizontal tail surface only.
[c] Subscript s is for full size.

RADIATING CHART OF VARIABLES

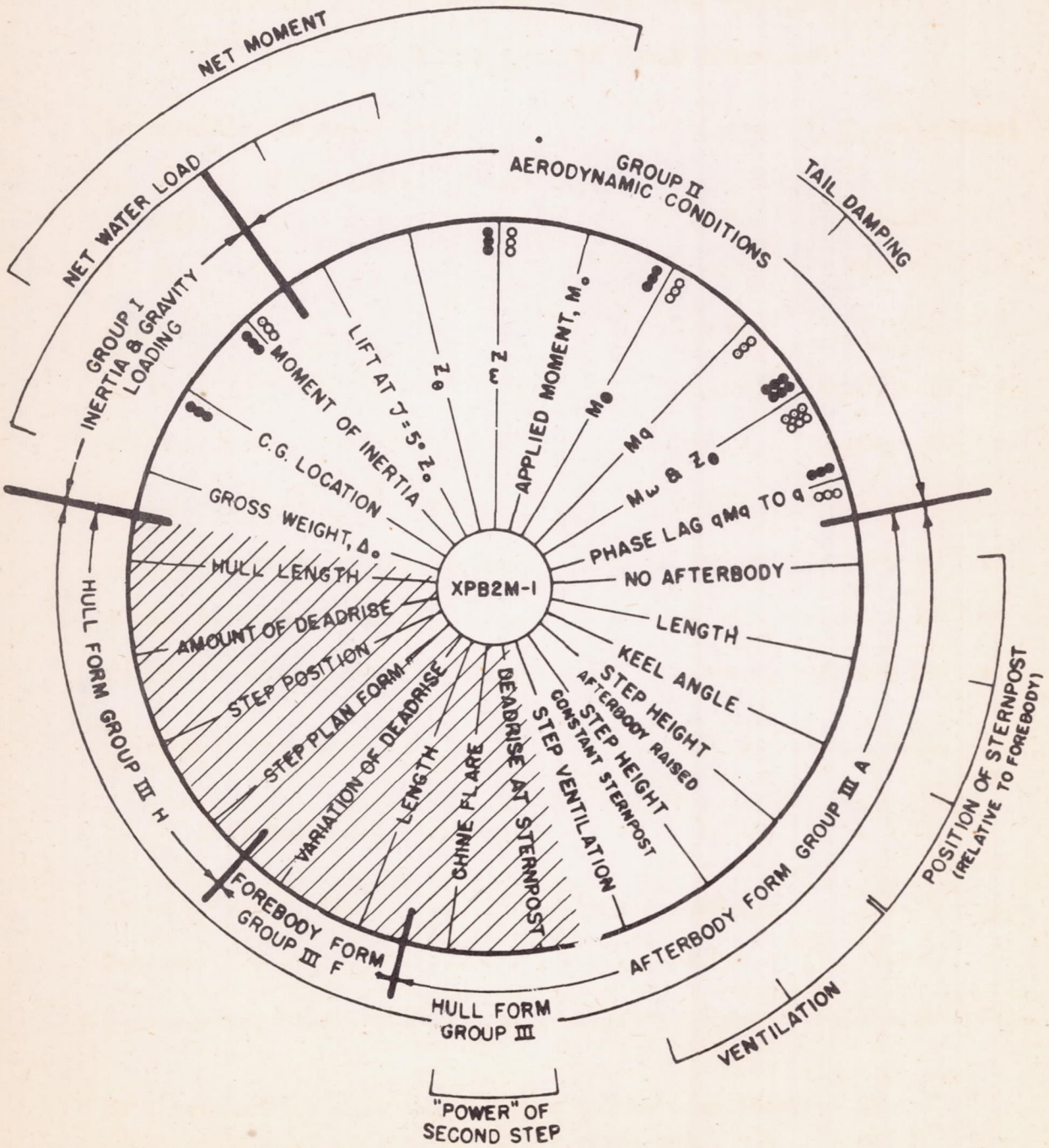

Figure 1.-

ooo no effect on steady-motion resistance characteristics.

●●● little or no effect on porpoising characteristics.

NACA CHART 1 GROUP I - WEIGHT AND INERTIA LOADING Fig. 2 a

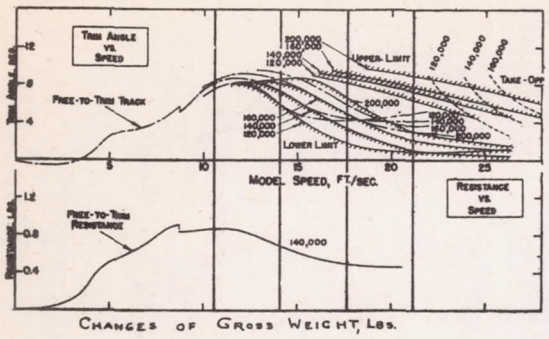

CHANGES OF GROSS WEIGHT, LBS.

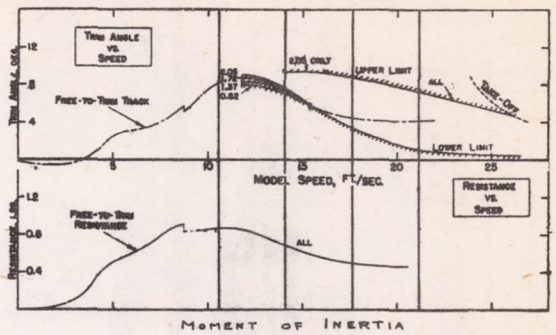

MOMENT OF INERTIA

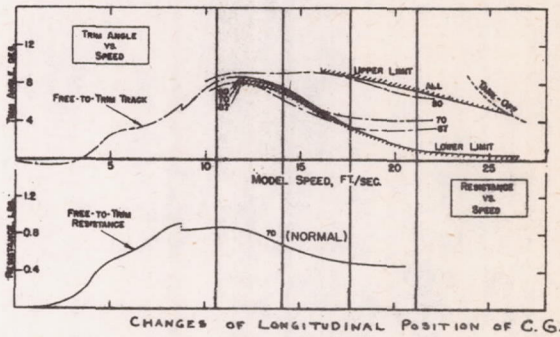

CHANGES OF LONGITUDINAL POSITION OF C.G.

W-68

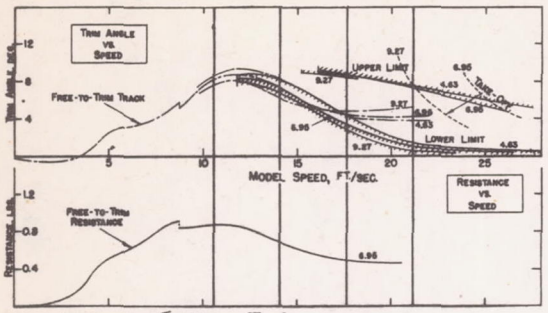

WING LIFT AT $f=5°$, Z_o

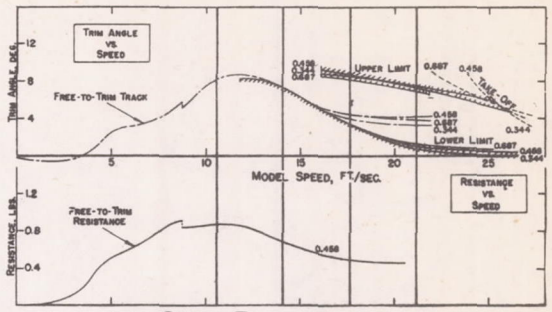

WING LIFT RATE, Z_θ

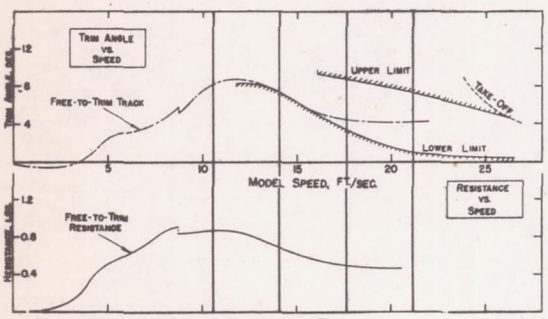

VERTICAL VELOCITY DAMPING, Z_w

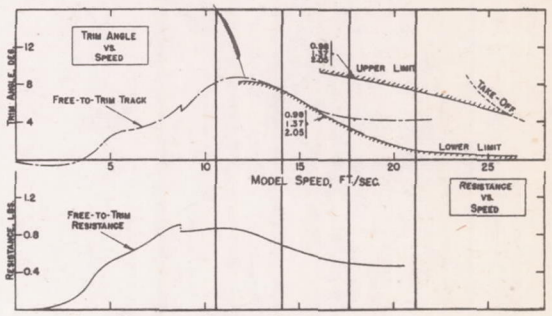

TAIL MOMENT RATE, M_θ

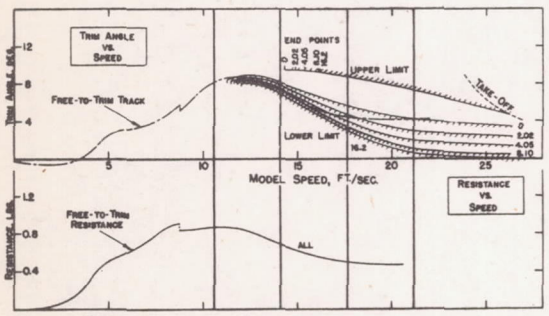

TAIL DAMPING, M_q,

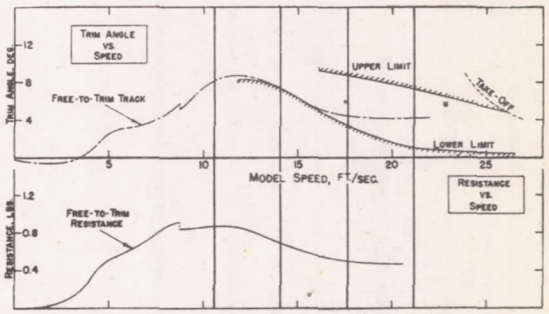

INTRODUCTION OF 35° LAGGING PHASE ANGLE BETWEEN qM_q AND q

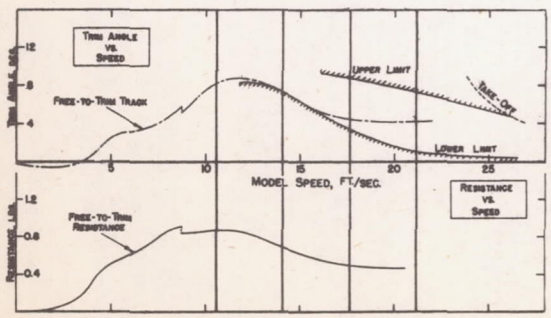

INCLUSION OF M_w & Z_q WITH M_q, COMPARED TO M_q ALONE

W-68

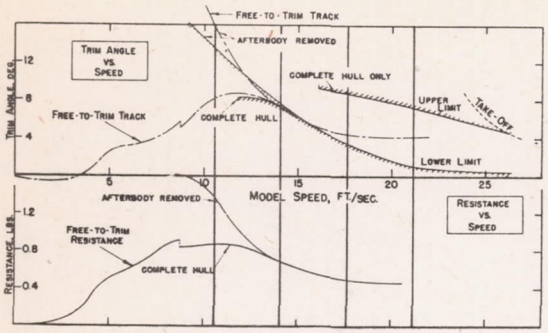

AFTERBODY REMOVED

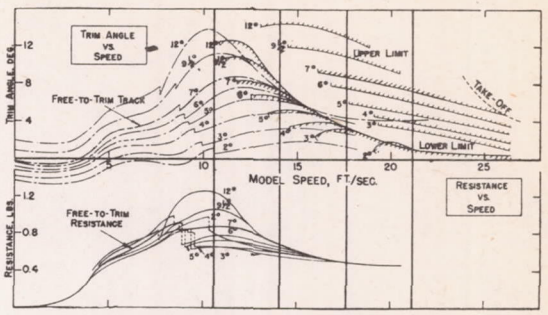

ANGLE BETWEEN FORE AND AFTERBODY KEELS

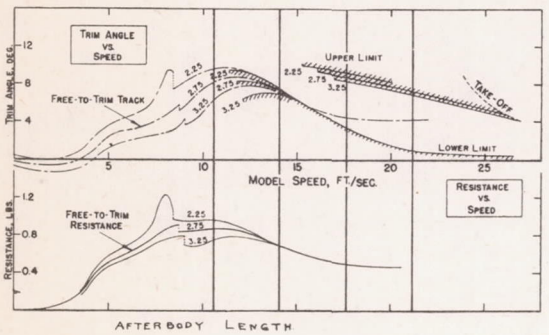

AFTERBODY LENGTH

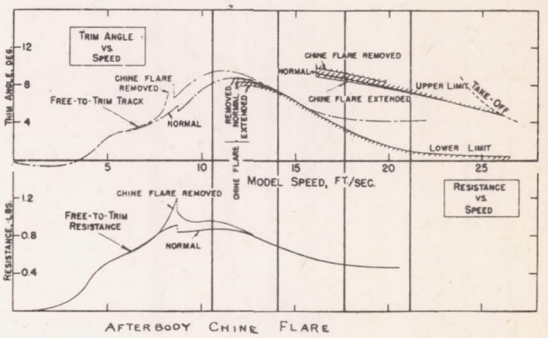

AFTERBODY CHINE FLARE

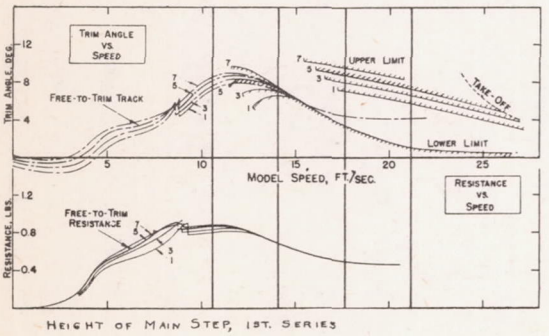

HEIGHT OF MAIN STEP, 1ST. SERIES

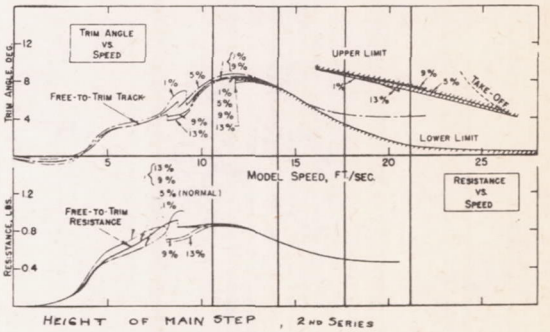

HEIGHT OF MAIN STEP, 2ND SERIES

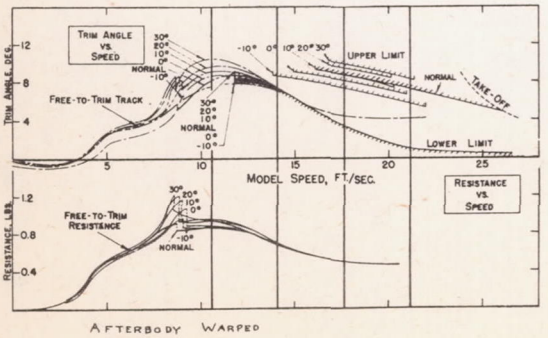

AFTERBODY WARPED

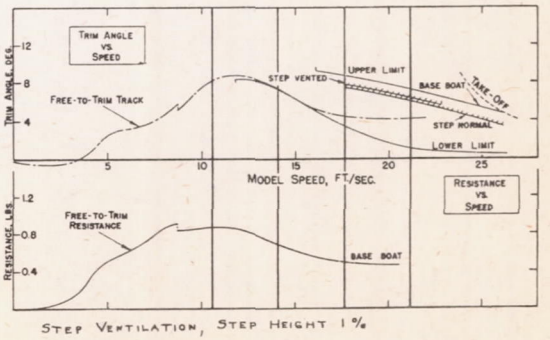

STEP VENTILATION, STEP HEIGHT 1%

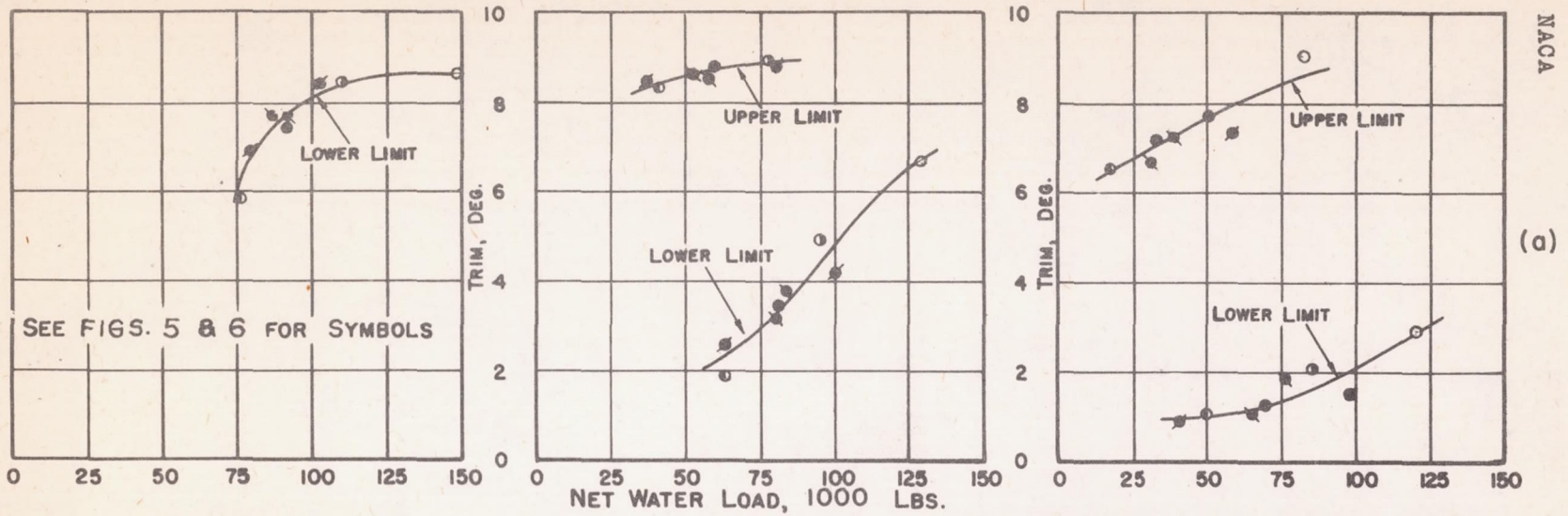

STABILITY LIMITS AS FUNCTIONS OF NET WATER LOAD FOR EXPERIMENTS ON Δ_0, Z_0, Z_g

$C_v = 3.71$ (14.13 fps) — $C_v = 4.64$ (17.65 fps) — $C_v = 5.57$ (21.18 fps)

(a)

CHANGES OF APPLIED MOMENT CORRESPONDING TO SHIFT OF C.G.

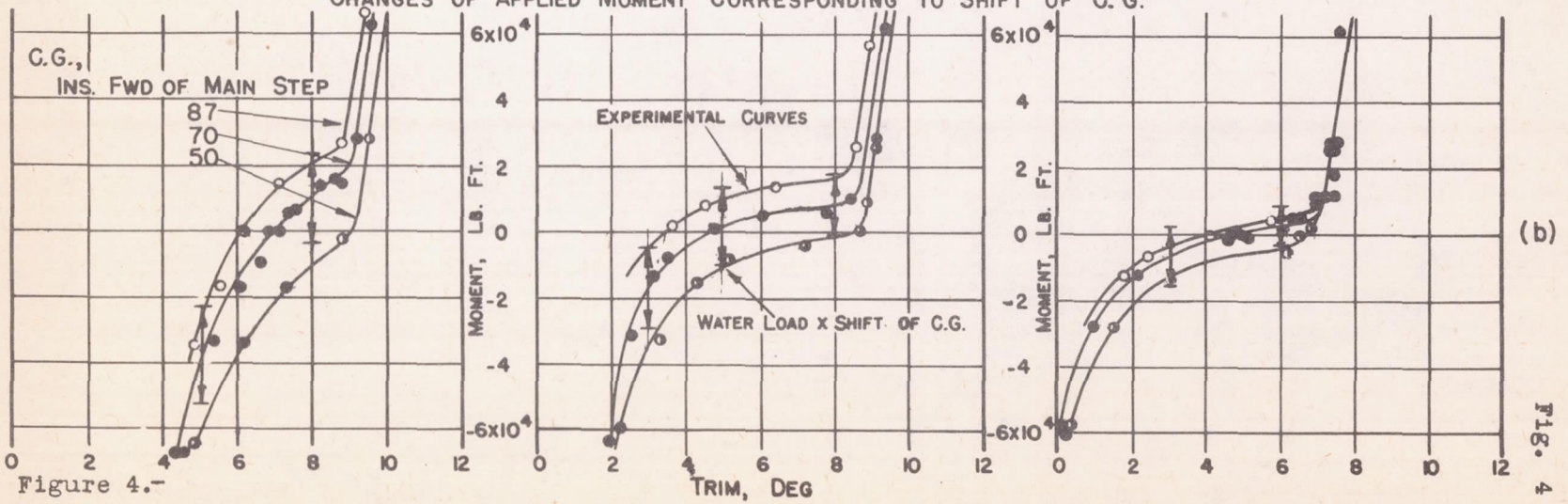

(b)

Figure 4.-

NACA Fig. 4

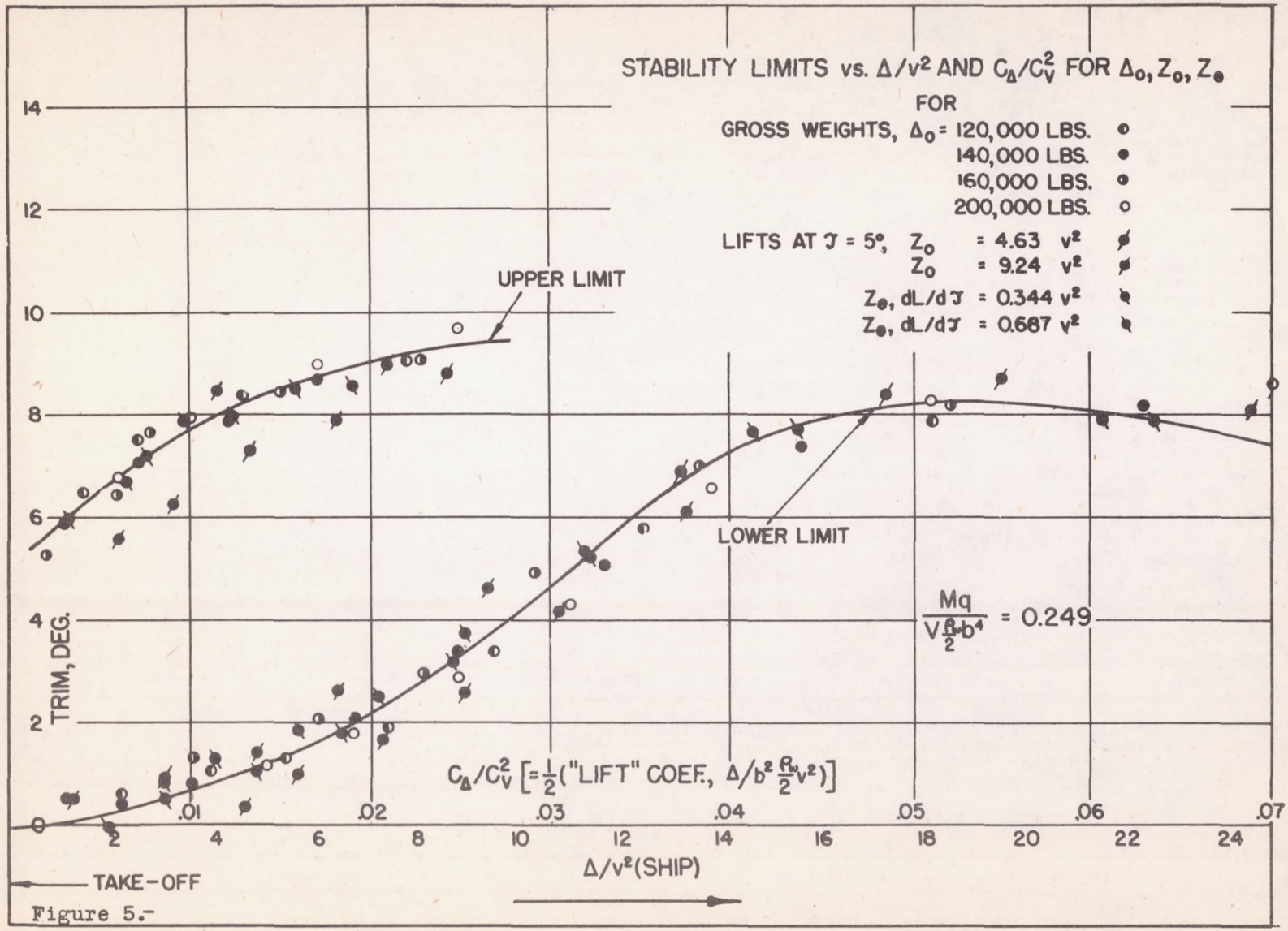

Figure 5.-

NACA Fig. 5

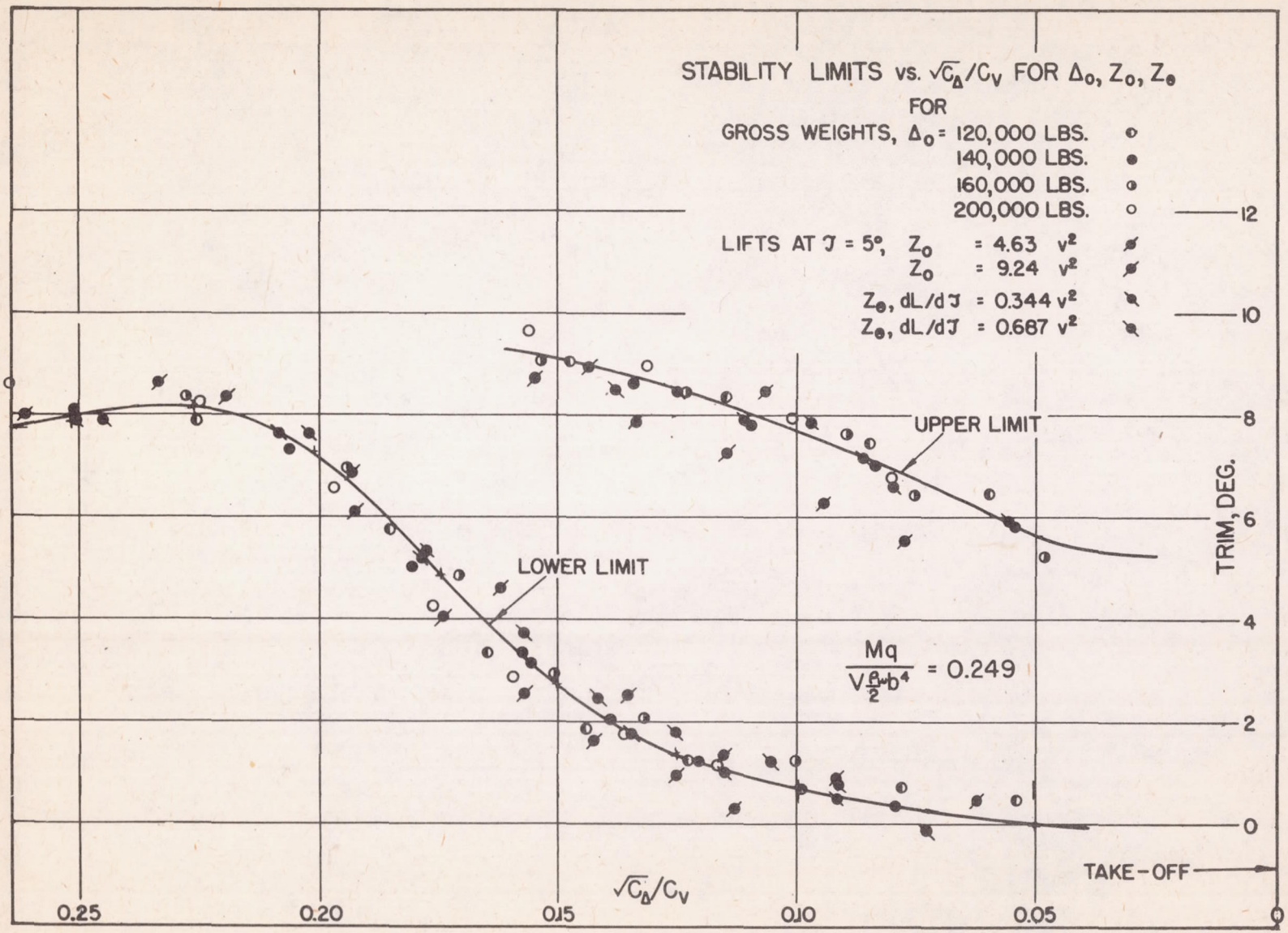
STABILITY LIMITS vs. $\sqrt{C_\Delta}/C_V$ FOR Δ_o, Z_o, Z_θ
FOR
GROSS WEIGHTS, Δ_o = 120,000 LBS.
140,000 LBS.
160,000 LBS.
200,000 LBS.
LIFTS AT τ = 5°, Z_o = 4.63 v^2
Z_o = 9.24 v^2
Z_θ, $dL/d\tau$ = 0.344 v^2
Z_θ, $dL/d\tau$ = 0.687 v^2
UPPER LIMIT
LOWER LIMIT
$\frac{Mq}{V\frac{\rho}{2}b^4}$ = 0.249
TRIM, DEG.
12
10
8
6
4
2
0
TAKE-OFF
$\sqrt{C_\Delta}/C_V$
0.25
0.20
0.15
0.10
0.05
0

NACA

Fig. 6

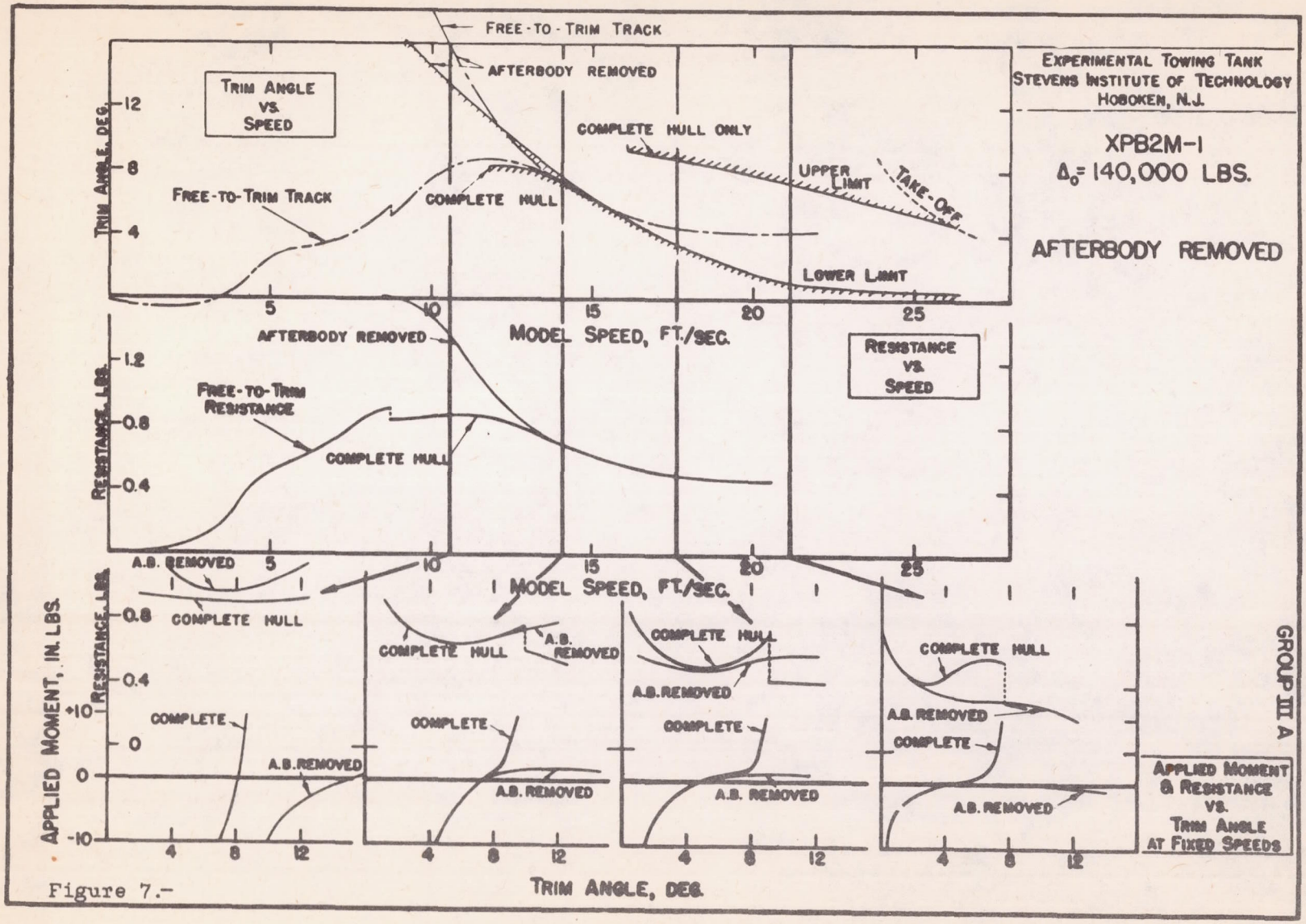

Figure 7.-

NACA GROUP III A Fig. 7

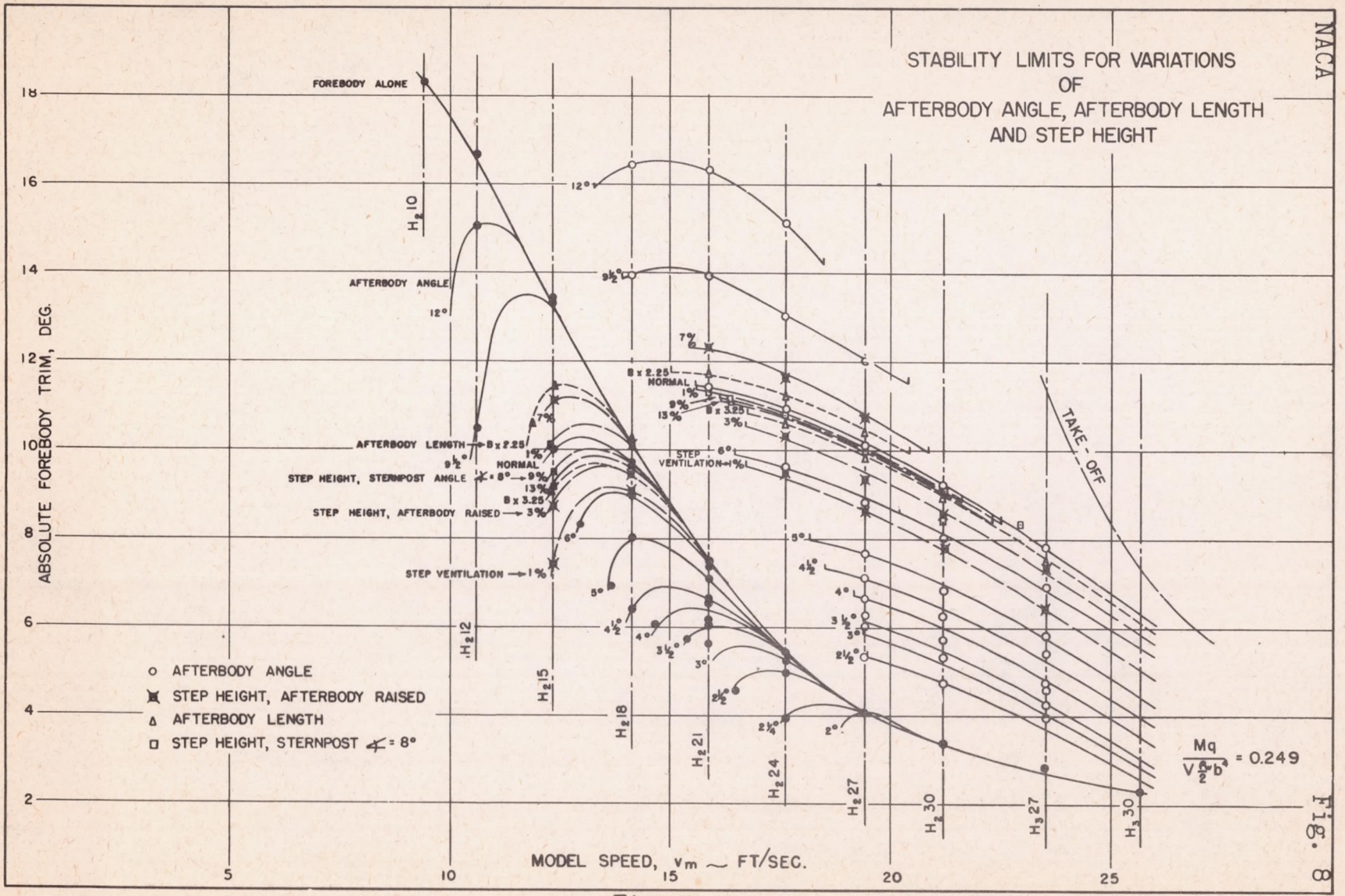
NACA
STABILITY LIMITS FOR VARIATIONS
OF
AFTERBODY ANGLE, AFTERBODY LENGTH
AND STEP HEIGHT
ABSOLUTE FOREBODY TRIM, DEG.
MODEL SPEED, V_m ~ FT/SEC.
FOREBODY ALONE
AFTERBODY ANGLE
AFTERBODY LENGTH → 8 x 2.25
NORMAL
STEP HEIGHT, STERNPOST ANGLE → 8°
STEP HEIGHT, AFTERBODY RAISED → 3%
8 x 3.25
STEP VENTILATION → 1%
TAKE-OFF
H_z10
H_z12
H_z15
H_z18
H_z21
H_z24
H_z27
H_z30
$H_3$27
$H_3$30
○ AFTERBODY ANGLE
✕ STEP HEIGHT, AFTERBODY RAISED
△ AFTERBODY LENGTH
□ STEP HEIGHT, STERNPOST ∠ = 8°
$\frac{Mq}{V\frac{\rho}{2}b^4}$ = 0.249
Fig. 8

Figure 8.-

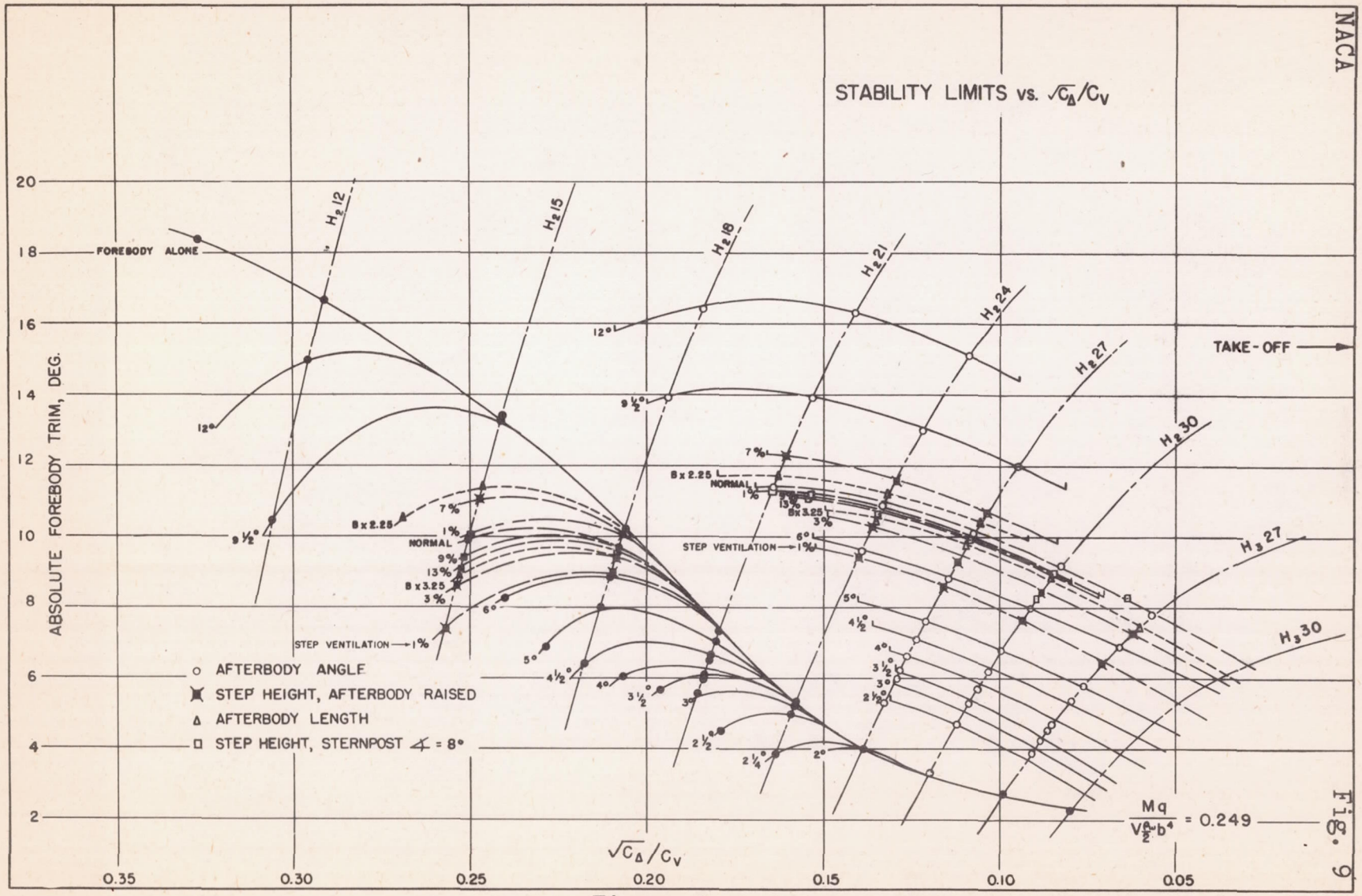
STABILITY LIMITS vs. $\sqrt{C_\Delta}/C_V$
NACA
ABSOLUTE FOREBODY TRIM, DEG.
$\sqrt{C_\Delta}/C_V$
FOREBODY ALONE
H_2 12
H_2 15
H_2 18
H_2 21
H_2 24
H_2 27
H_3 30
H_3 27
H_3 30
TAKE-OFF
STEP VENTILATION → 1%
8 x 2.25
NORMAL
8 x 3.25
○ AFTERBODY ANGLE
✖ STEP HEIGHT, AFTERBODY RAISED
△ AFTERBODY LENGTH
□ STEP HEIGHT, STERNPOST ∠ = 8°
$\frac{Mq}{V\frac{\rho}{2}b^4}$ = 0.249
Fig. 9

Figure 9.-

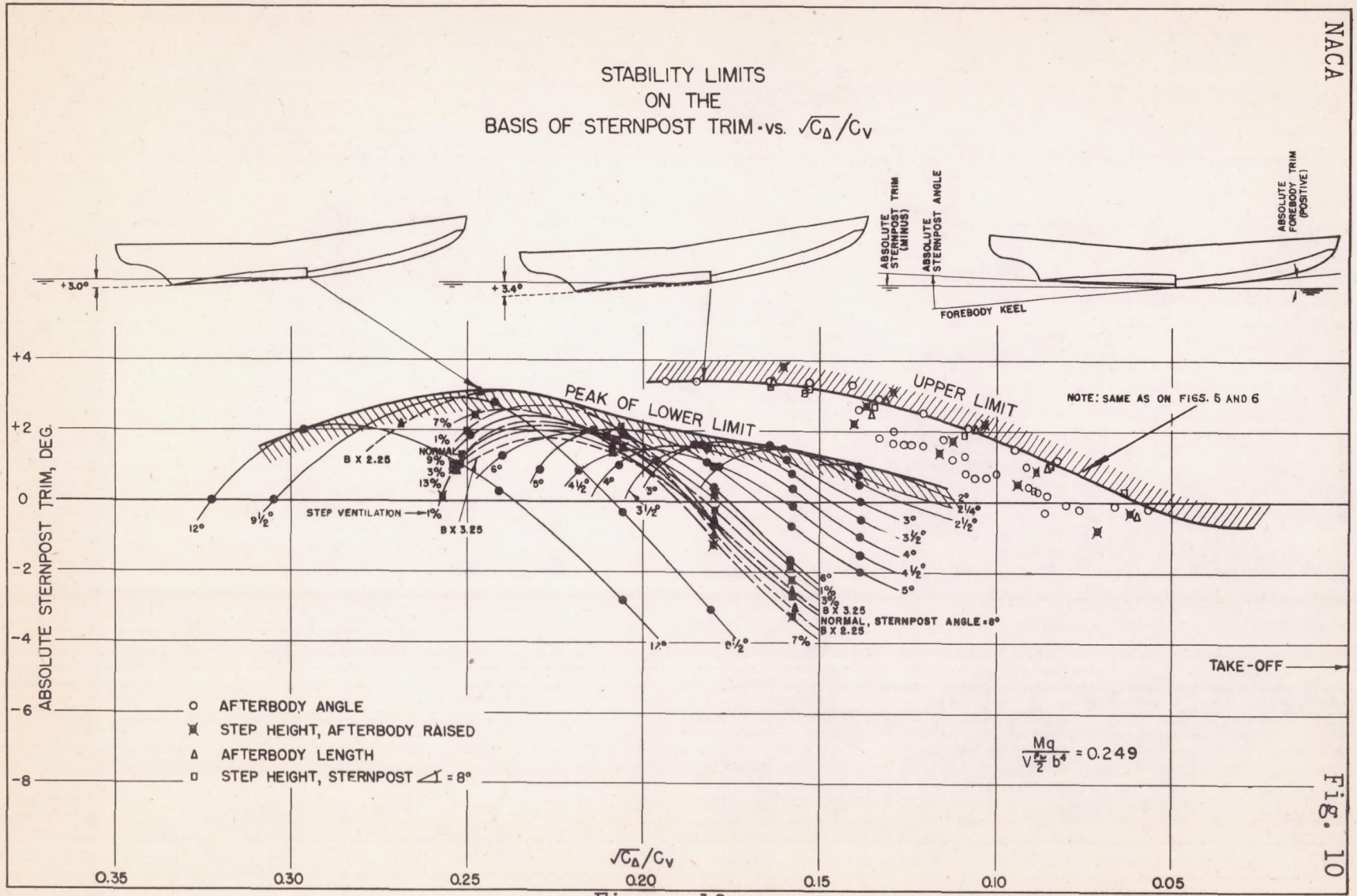
STABILITY LIMITS
ON THE
BASIS OF STERNPOST TRIM vs. $\sqrt{C_\Delta}/C_V$
NACA
+3.0°
+3.4°
ABSOLUTE STERNPOST TRIM (MINUS)
ABSOLUTE STERNPOST ANGLE
ABSOLUTE FOREBODY TRIM (POSITIVE)
FOREBODY KEEL
PEAK OF LOWER LIMIT
UPPER LIMIT
NOTE: SAME AS ON FIGS. 5 AND 6
B X 2.25
B X 3.25
STEP VENTILATION
NORMAL, STERNPOST ANGLE = 8°
TAKE-OFF
ABSOLUTE STERNPOST TRIM, DEG.
+4
+2
0
-2
-4
-6
-8
AFTERBODY ANGLE
STEP HEIGHT, AFTERBODY RAISED
AFTERBODY LENGTH
STEP HEIGHT, STERNPOST ∠ = 8°
$\frac{Mq}{V\frac{\rho}{2}b^4} = 0.249$
$\sqrt{C_\Delta}/C_V$
0.35
0.30
0.25
0.20
0.15
0.10
0.05
Fig. 10

Figure 10.-

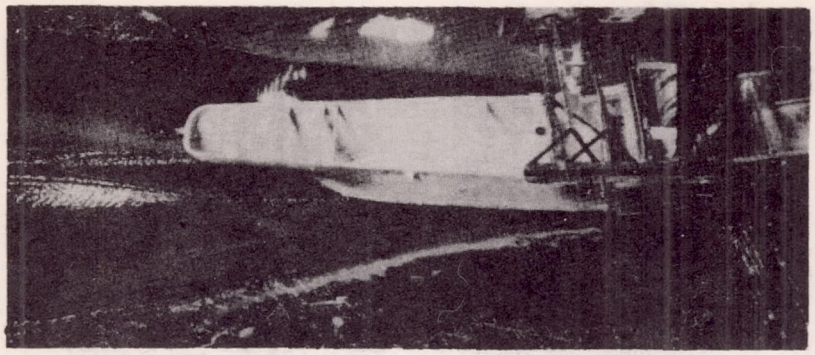

Afterbody angle = 12°

Stern-post angle = 13°

Abs. forebody trim = 13.4°

Abs. stern-post trim = 0.4°

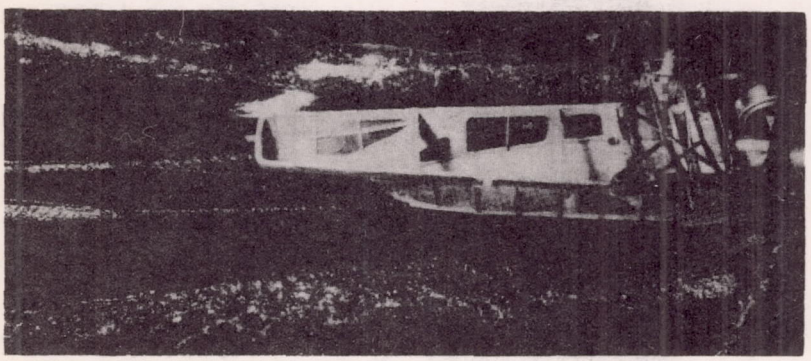

Afterbody angle = 7°

Stern-post angle = 8°

Abs. forebody trim = 8.7°

Abs. stern-post trim = 0.7°

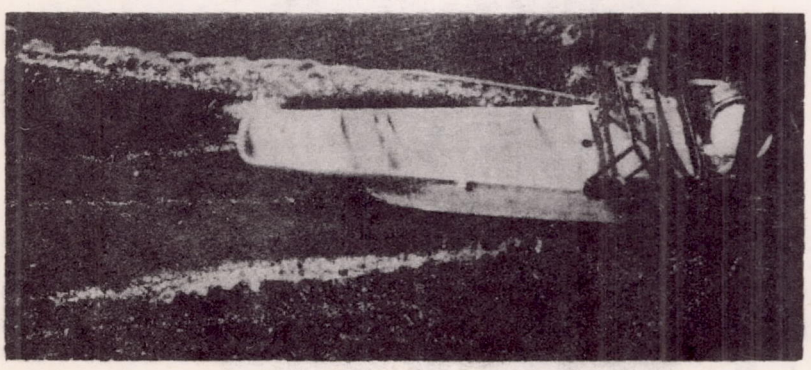

Afterbody angle = 4.5°

Stern-post angle = 5.5°

Abs. forebody trim = 5.5°

Abs. stern-post trim = 0.0°

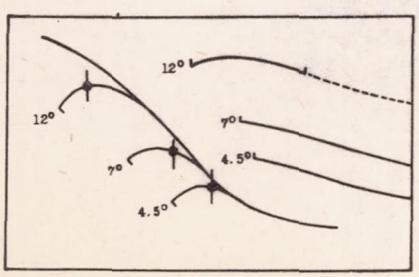

Afterbody angle, deg	$\sqrt{\Delta/\nabla^2}$	$\sqrt{C_\Delta}/C_\nabla$
12	1.02	0.298
7	.766	.224
4.5	.620	.181

(a)

Figure 11.- Steady-motion photographs at lower limit, peak of "breakaway".

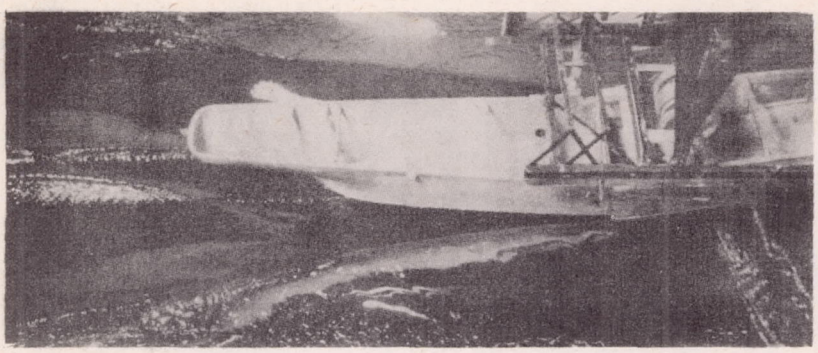

Afterbody angle = 12°

Stern-post angle = 13°

Abs. forebody trim = 14.4°

Abs. stern-post trim = 1.4°

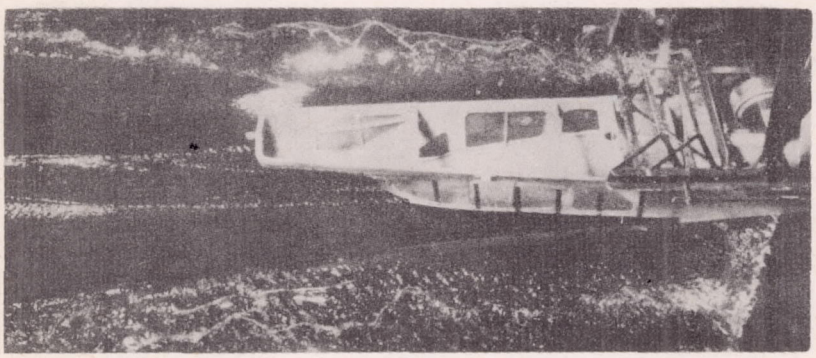

Afterbody angle = 7°

Stern-post angle = 8°

Abs. forebody trim = 9.7°

Abs. stern-post trim = 1.7°

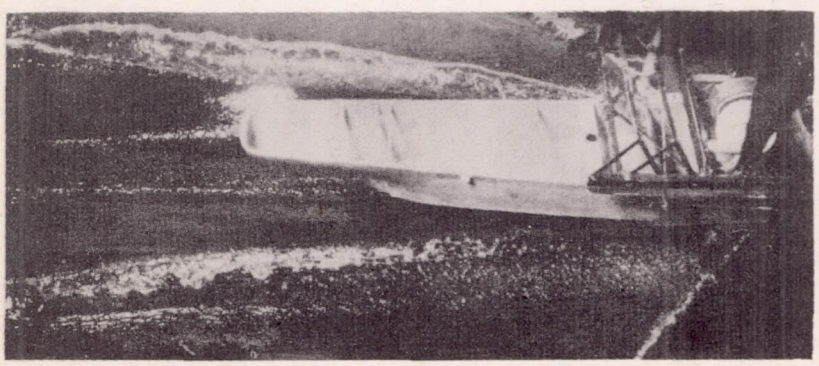

Afterbody angle = 4.5°

Stern-post angle = 5.5°

Abs. forebody trim = 6.5°

Abs. stern-post trim = 1.0°

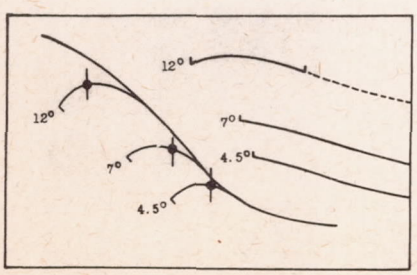

Afterbody angle, deg	$\sqrt{\Delta/v^2}$	$\sqrt{C_\Delta/C_V}$
12	1.02	0.298
7	.766	.224
4.5	.620	.181

(b)

Figure 11.- Continued.

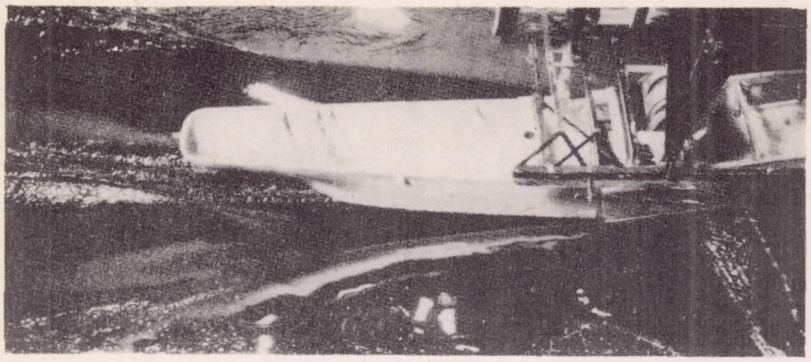

Afterbody angle = 12°

Stern-post angle = 13°

Abs. forebody trim = 15.4°

Abs. stern-post trim = 2.4°

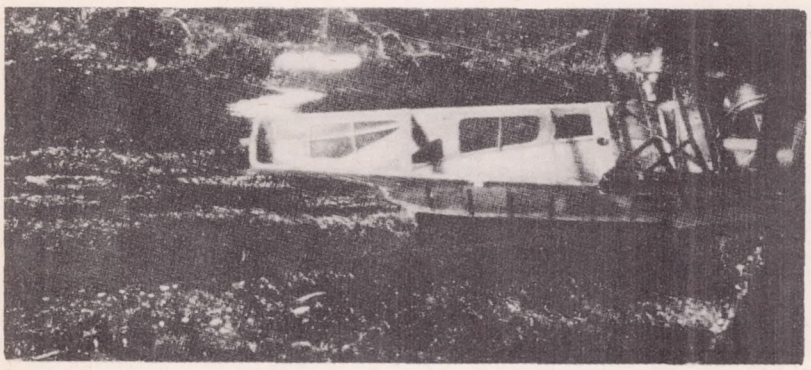

Afterbody angle = 7°

Stern-post angle = 8°

Abs. forebody trim = 10.7°

Abs. stern-post trim = 2.7°

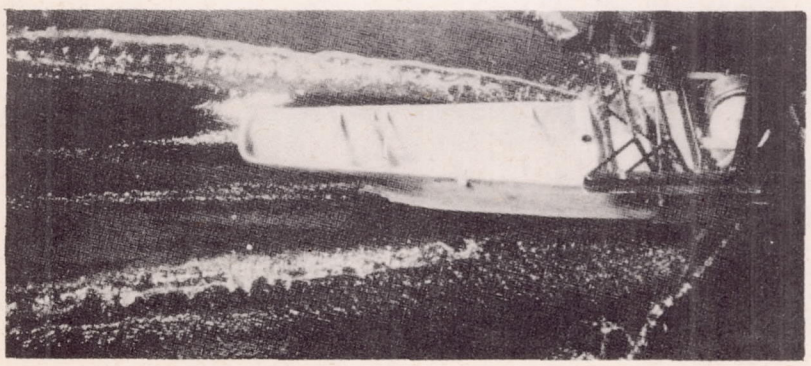

Afterbody angle = 4.5°

Stern-post angle = 5.5°

Abs. forebody trim = 7.5°

Abs. stern-post trim = 2°

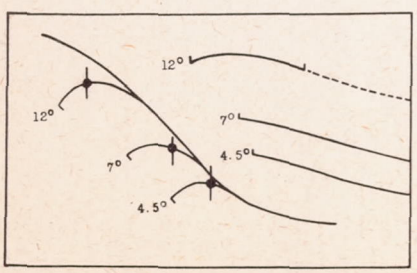

Afterbody angle, deg	$\sqrt{\Delta/v^2}$	$\sqrt{C_\Delta}/C_V$
12	1.02	0.298
7	.766	.224
4.5	.620	.181

(c)

Figure 11.- Concluded.

W-68

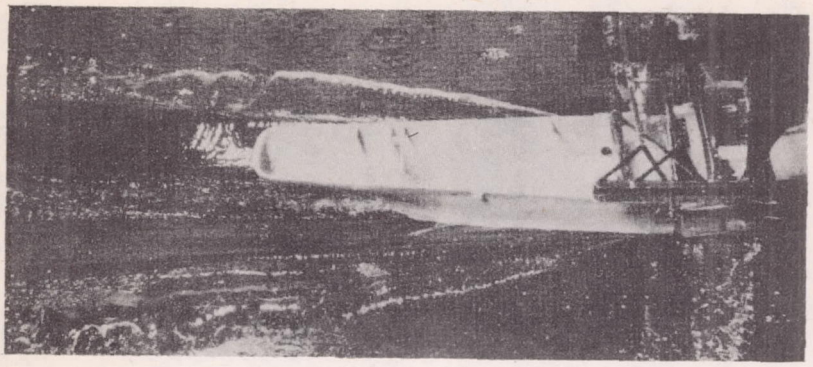

Afterbody angle = 12°

Stern-post angle = 13°

Abs. forebody trim = 15.4°

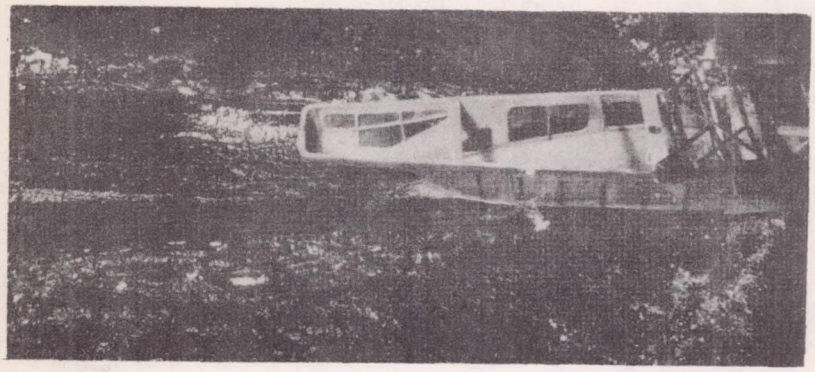

Afterbody angle = 7°

Stern-post angle = 8°

Abs. forebody trim = 10.4°

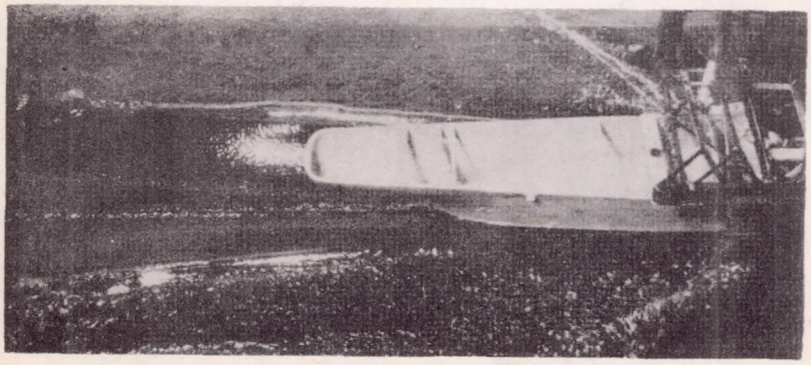

Afterbody angle = 4.5°

Stern-post angle = 5.5°

Abs. forebody trim = 7.9°

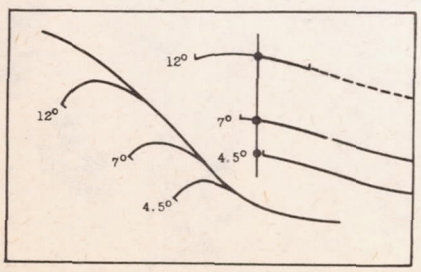

$\sqrt{\Delta}/v^2 = 0.493$, $\sqrt{C_\Delta}/C_V = 0.143$

(a) Absolute stern-post trim, 2.4°.

Figure 12.- Steady-motion photographs at upper limit, moderate planing speed

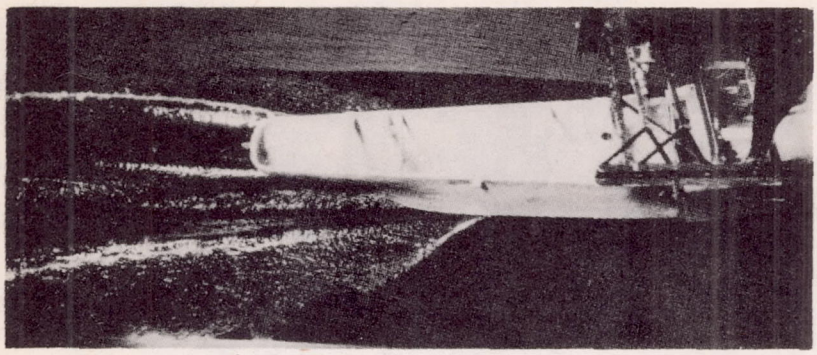

Afterbody angle = 12°

Stern-post angle = 13°

Abs. forebody trim = 16.4°

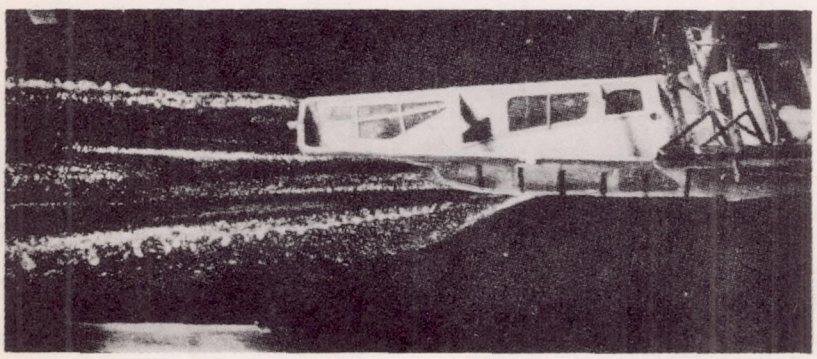

Afterbody angle = 7°

Stern-post angle = 8°

Abs. forebody trim = 11.4°

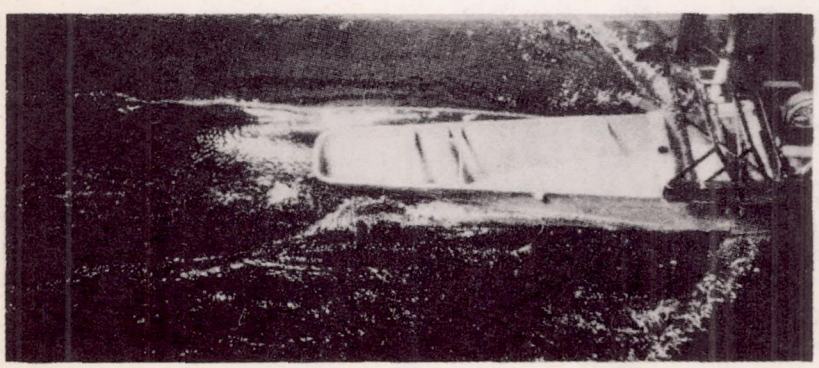

Afterbody angle = 4.5°

Stern-post angle = 5.5°

Abs. forebody trim = 8.9°

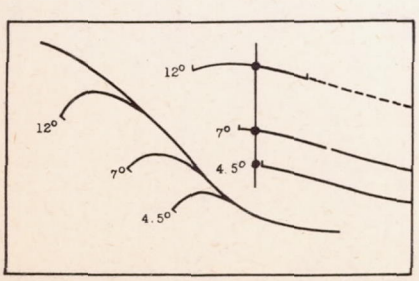

$\sqrt{\Delta/v^2} = 0.493$, $\sqrt{C_\Delta}/C_V = 0.143$

(b) Absolute stern-post trim, 3.4°.

Figure 12.- Continued.

W-68

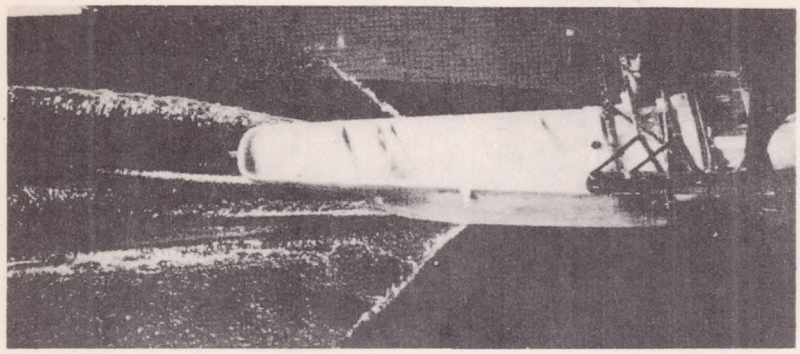

Afterbody angle = 12°

Stern-post angle = 13°

Abs. forebody trim = 17.4°

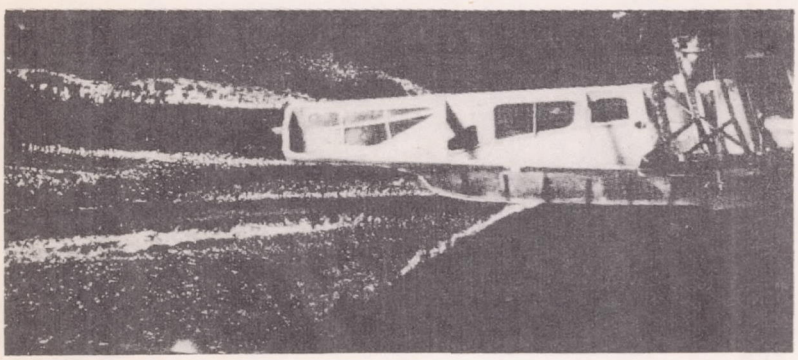

Afterbody angle = 7°

Stern-post angle = 8°

Abs. forebody trim = 12.4°

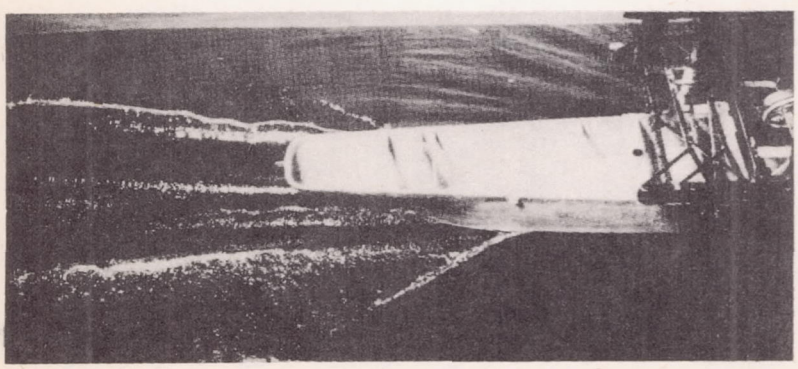

Afterbody angle = 4.5°

Stern-post angle = 5.5°

Abs. forebody trim = 9.9°

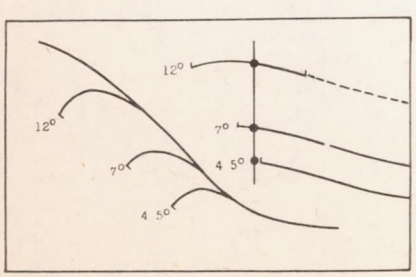

$\sqrt{\Delta}/v^2 = 0.493$, $\sqrt{C_\Delta}/C_V = 0.143$

(c) Absolute stern-post trim, 4.4°.

Figure 12.- Concluded.

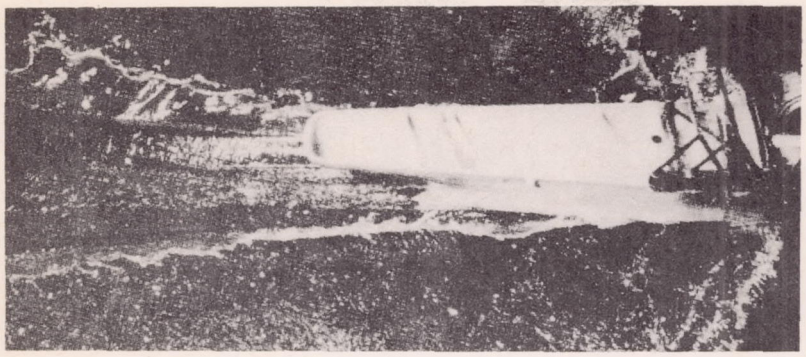

Afterbody angle = 12°

Stern-post angle = 13°

Abs. forebody trim = 13.2°

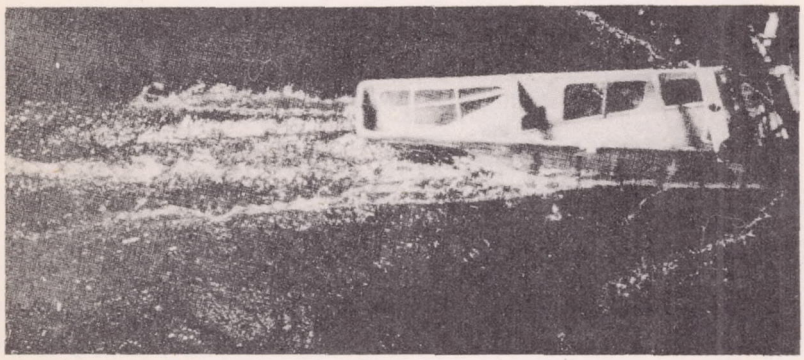

Afterbody angle = 7°

Stern-post angle = 8°

Abs. forebody trim = 8.2°

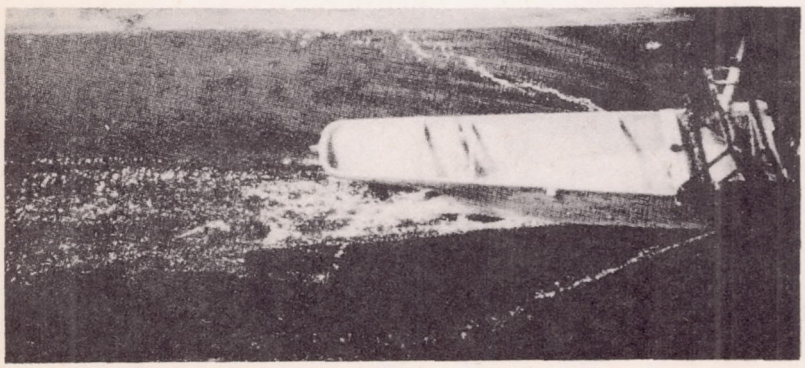

Afterbody angle = 4.5°

Stern-post angle = 5.5°

Abs. forebody trim = 5.7°

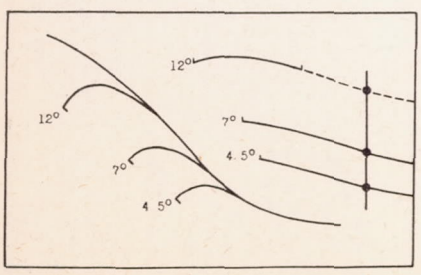

$\sqrt{\Delta}/v^2 = 0.146$, $\sqrt{C_\Delta}/C_V = 0.0425$

(a) Absolute stern-post trim, 0.2°.

Figure 13.- Steady-motion photographs at upper limit, high planing speeds.

W-68

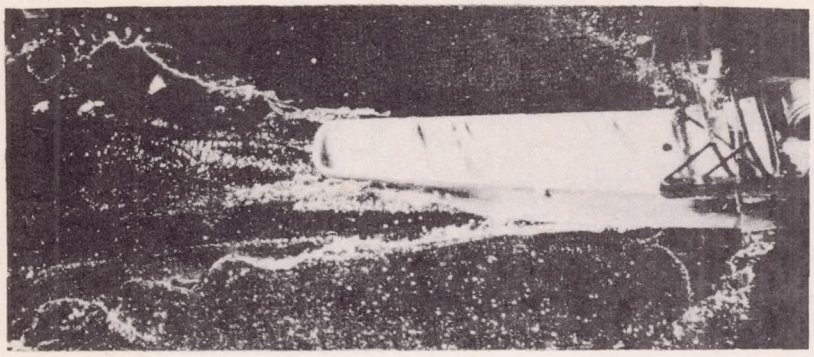

Afterbody angle = 12°

Stern-post angle = 13°

Abs. forebody trim = 14.2°

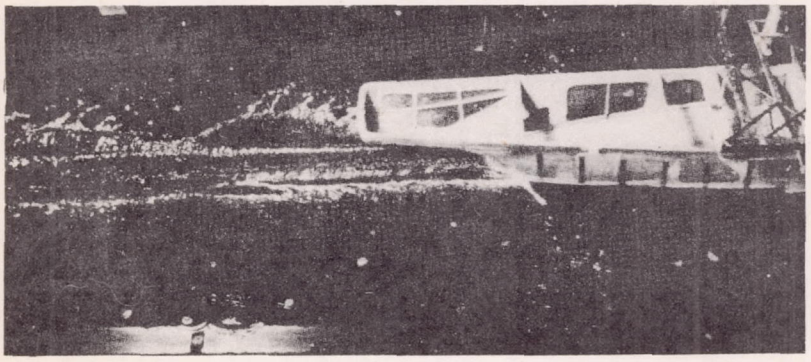

Afterbody angle = 7°

Stern-post angle = 8°

Abs. forebody trim = 9.2°

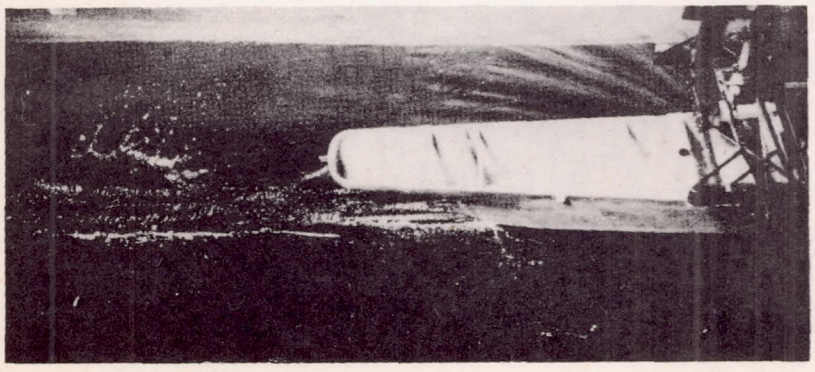

Afterbody angle = 4.5°

Stern-post angle = 5.5°

Abs. forebody trim = 6.7°

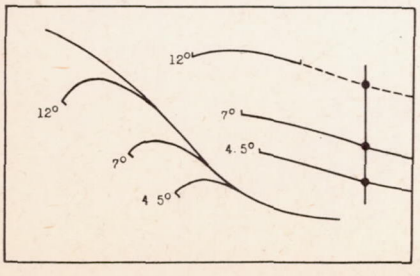

$\sqrt{\Delta/v^2} = 0.146$, $\sqrt{C_\Delta}/C_V = 0.0425$

(b) Absolute stern-post trim, 1.2°.

Figure 13.- Continued.

W-68

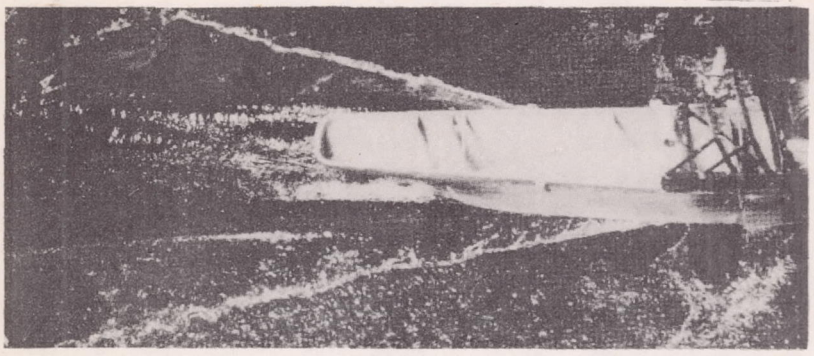

Afterbody angle = 12°

Stern-post angle = 13°

Abs. forebody trim = 15.2°

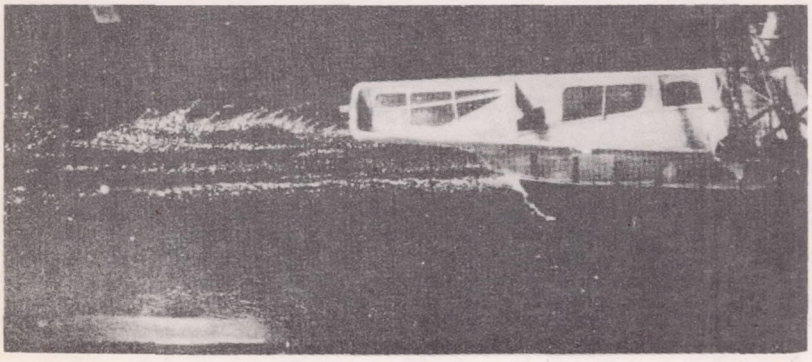

Afterbody angle = 7°

Stern-post angle = 8°

Abs. forebody trim = 10.2°

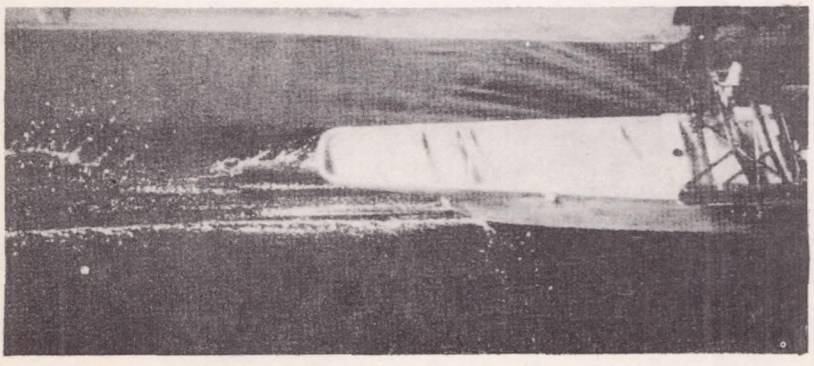

Afterbody angle = 4.5°

Stern-post angle = 5.5°

Abs. forebody trim = 7.7°

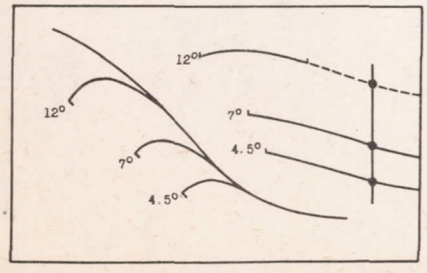

$\sqrt{\Delta/v^2} = 0.146$, $\sqrt{C_\Delta}/C_V = 0.0425$

(c) Absolute stern-post trim, 2.2°.

Figure 13.- Concluded.

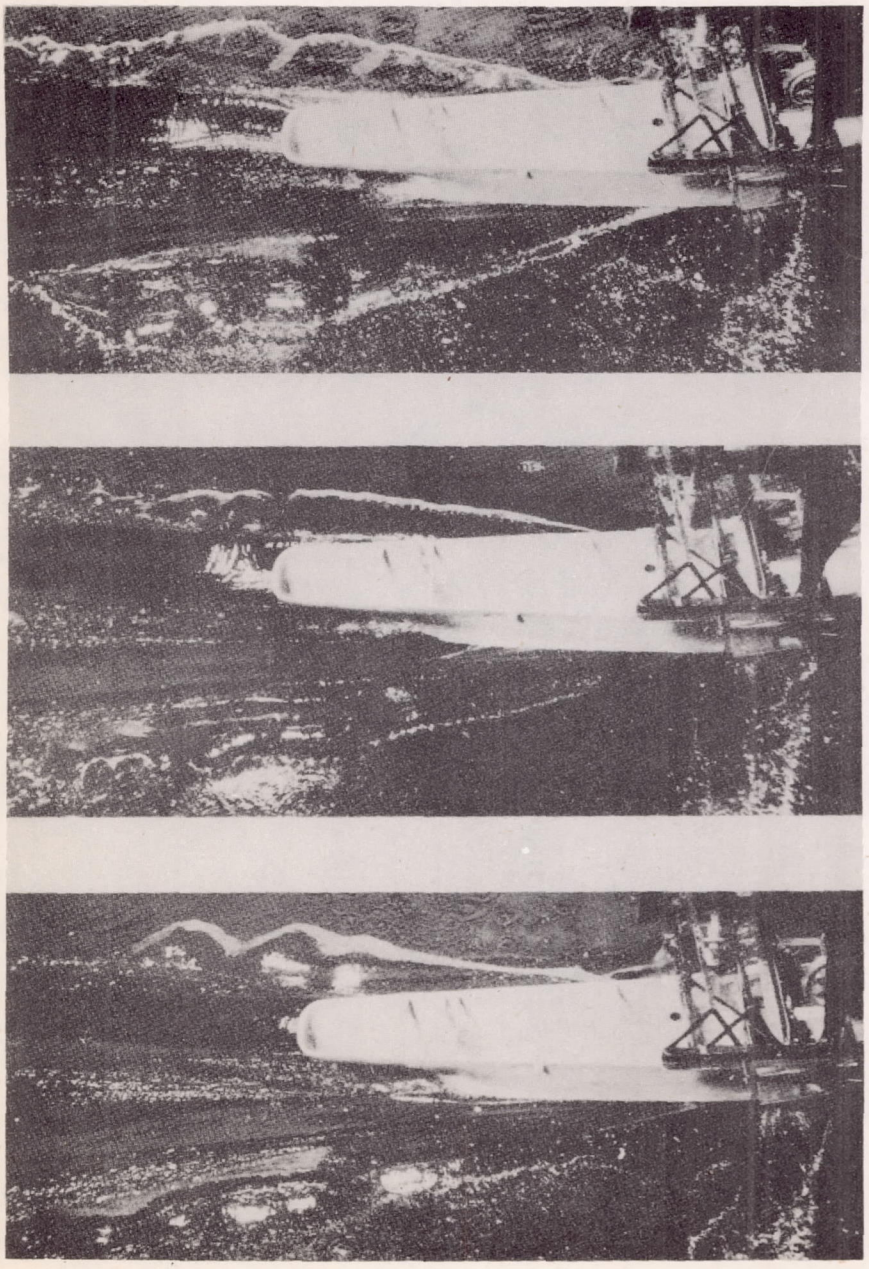

$C_V = 4.636$

$C_\Delta = 0.444$

$C_V = 4.173$

$C_\Delta = 0.361$

$C_V = 3.701$

$C_\Delta = 0.285$

(a) Absolute forebody trim, 15.4°.

Figure 14.- Steady-motion photographs to illustrate similarity of flow patterns at constant values of $\sqrt{C_\Delta}/C_V$ obtained with different combinations of C_Δ and C_V. Afterbody angle, 12°; $\sqrt{C_\Delta}/C_V = 0.144$.

W-68

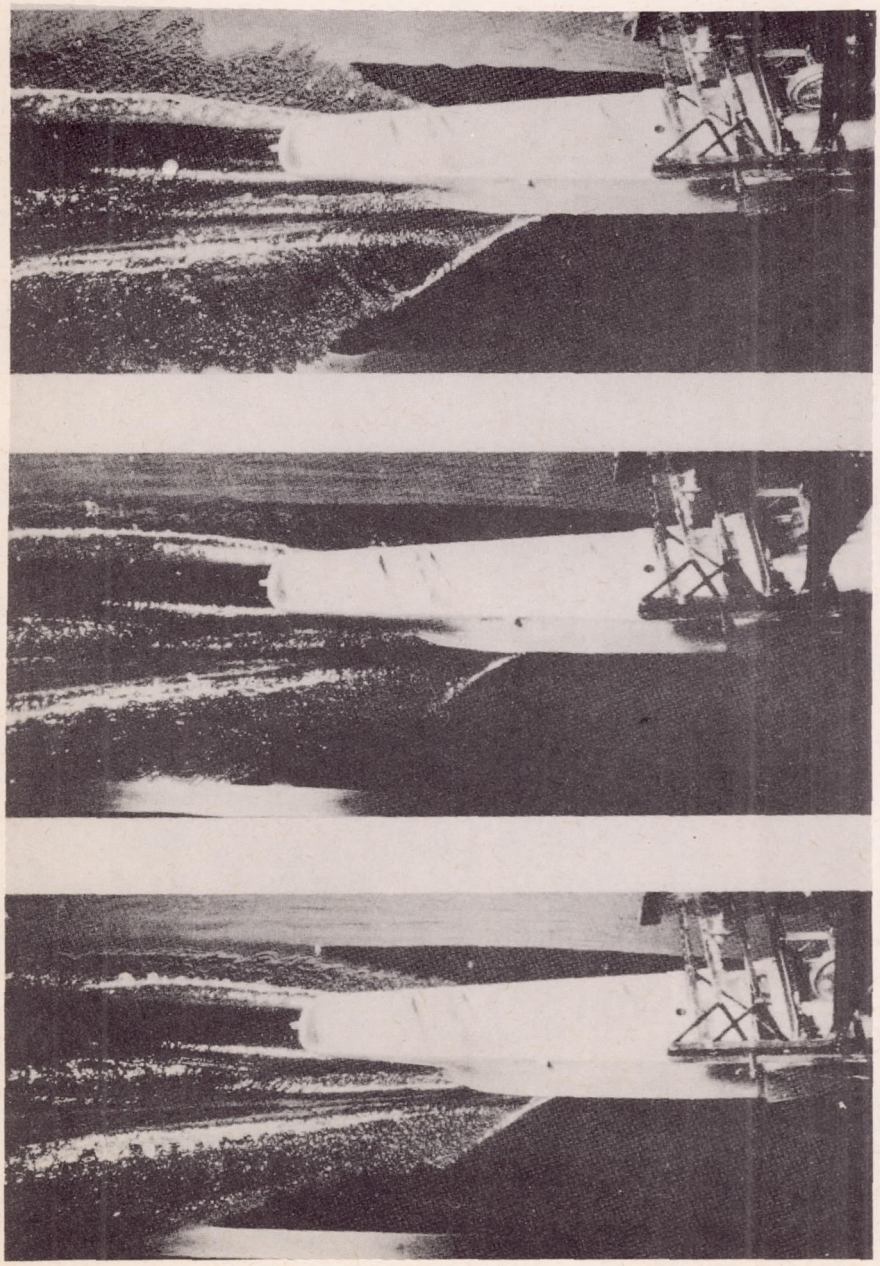

$C_V = 4.636$

$C_\Delta = 0.444$

$C_V = 4.173$

$C_\Delta = 0.361$

$C_V = 3.701$

$C_\Delta = 0.285$

(b) Absolute forebody trim, 16.4°.

Figure 14.- Continued.

W-89-M

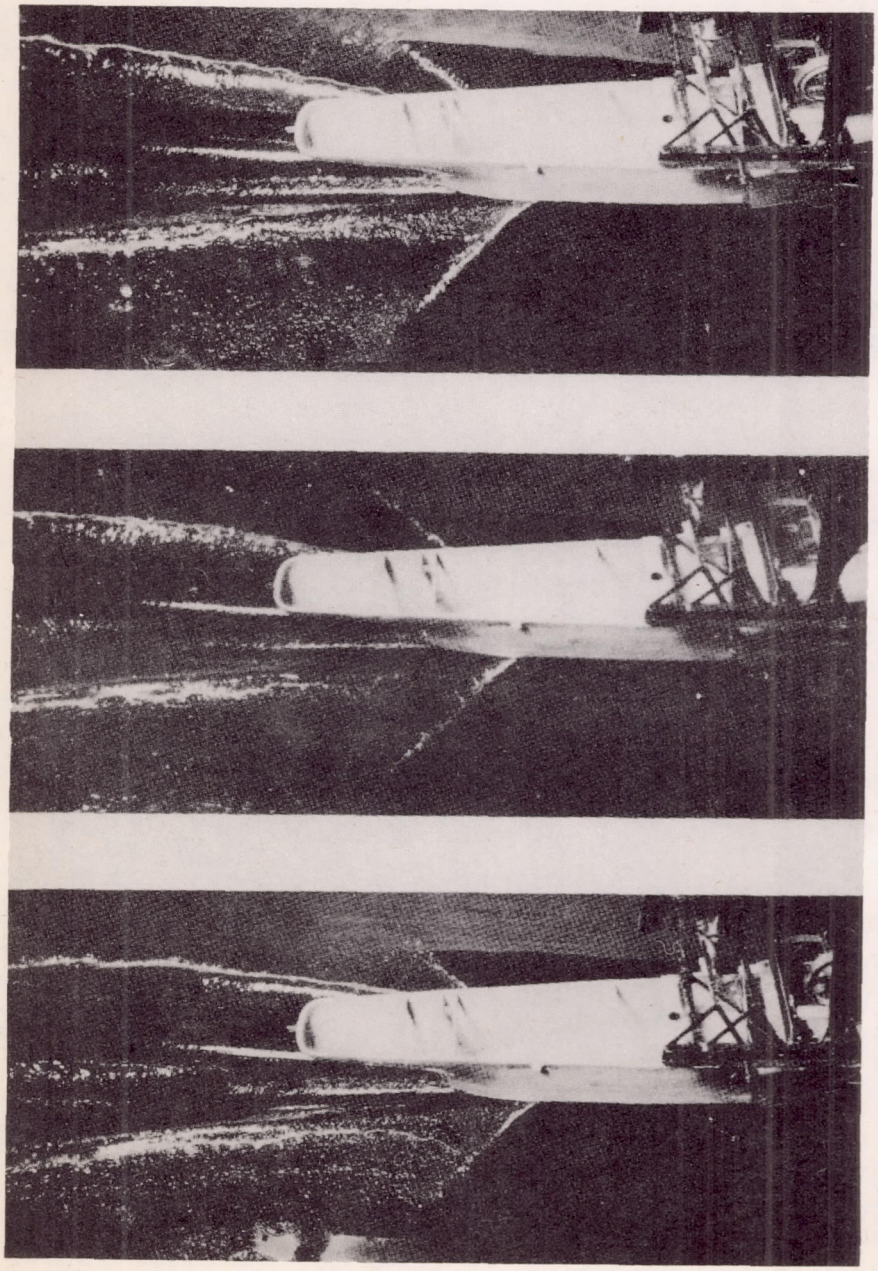

$C_V = 4.636$

$C_\Delta = 0.444$

$C_V = 4.173$

$C_\Delta = 0.361$

$C_V = 3.701$

$C_\Delta = 0.285$

(c) Absolute forebody trim, 17.4°.

Figure 14.- Concluded.

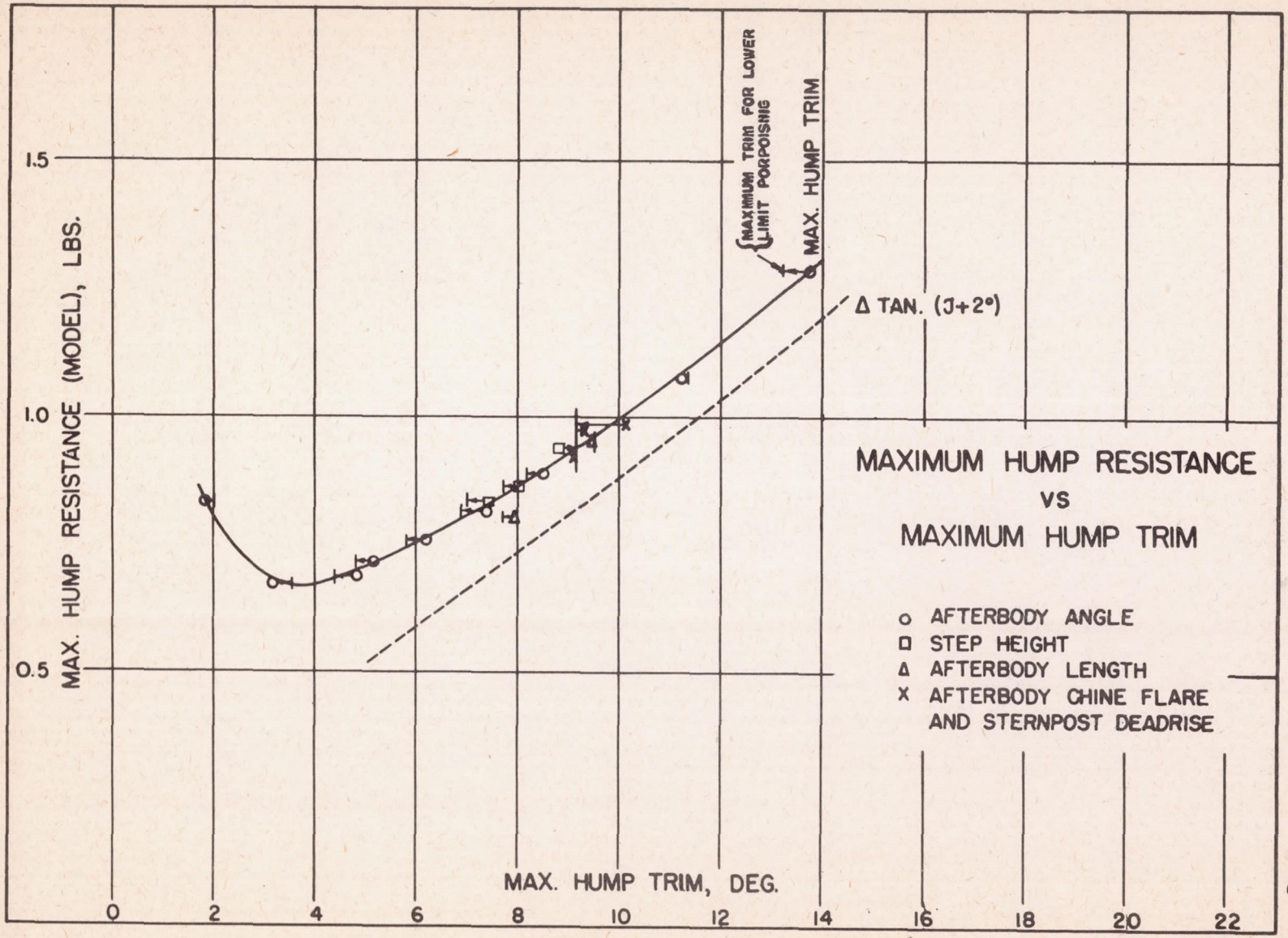
MAXIMUM HUMP RESISTANCE
VS
MAXIMUM HUMP TRIM
MAX. HUMP RESISTANCE (MODEL), LBS.
MAX. HUMP TRIM, DEG.
1.5
1.0
0.5
0
2
4
6
8
10
12
14
16
18
20
22
MAXIMUM TRIM FOR LOWER LIMIT PORPOISING
MAX. HUMP TRIM
Δ TAN. (J+2°)
o AFTERBODY ANGLE
□ STEP HEIGHT
Δ AFTERBODY LENGTH
X AFTERBODY CHINE FLARE AND STERNPOST DEADRISE

NACA

Fig. 15

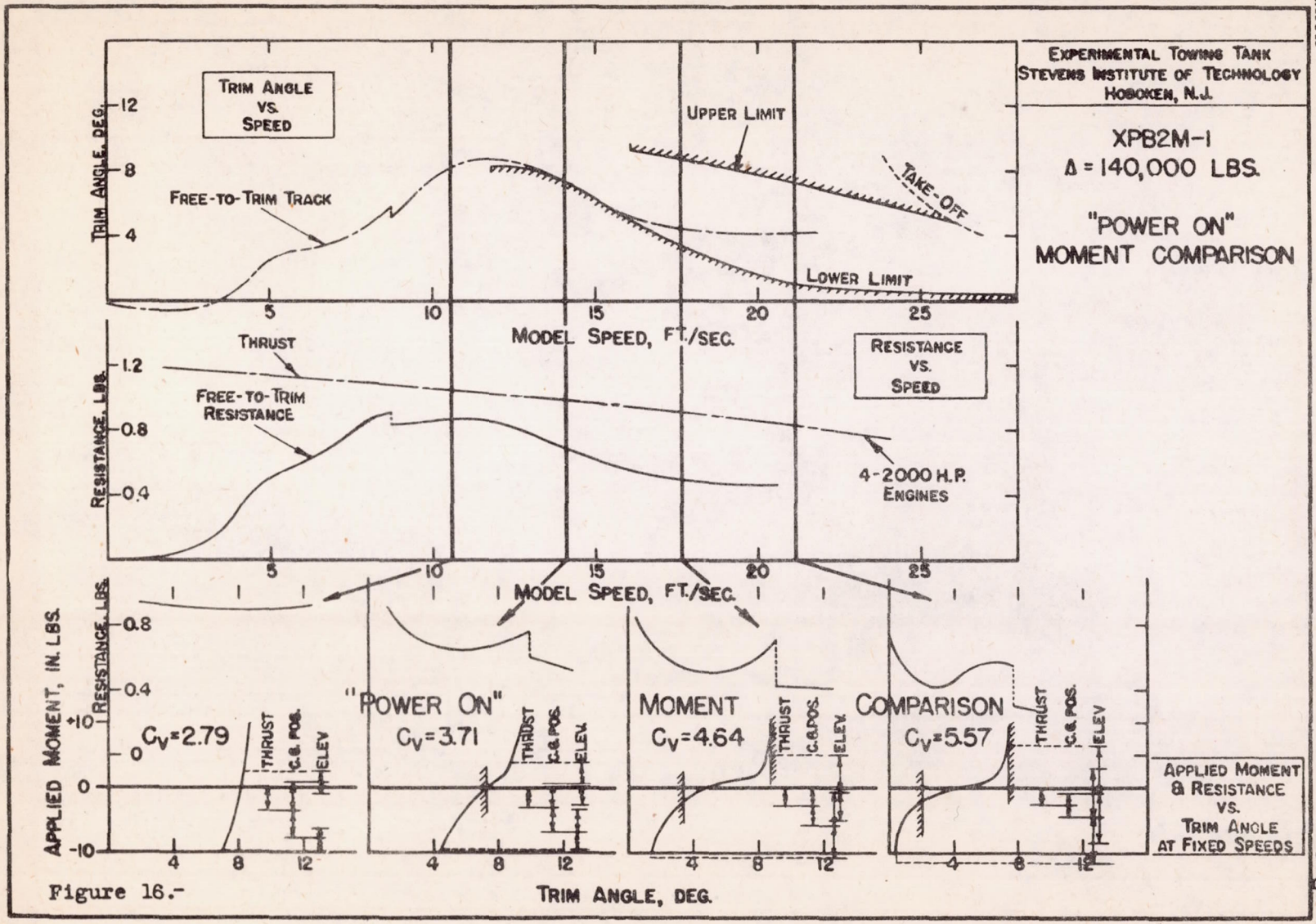
EXPERIMENTAL TOWING TANK
STEVENS INSTITUTE OF TECHNOLOGY
HOBOKEN, N.J.
XPB2M-1
Δ = 140,000 LBS.
"POWER ON"
MOMENT COMPARISON
TRIM ANGLE VS. SPEED
TRIM ANGLE, DEG.
FREE-TO-TRIM TRACK
UPPER LIMIT
TAKE-OFF
LOWER LIMIT
MODEL SPEED, FT./SEC.
RESISTANCE VS. SPEED
RESISTANCE, LBS.
THRUST
FREE-TO-TRIM RESISTANCE
4-2000 H.P. ENGINES
APPLIED MOMENT, IN. LBS.
"POWER ON" MOMENT COMPARISON
C_V=2.79
C_V=3.71
C_V=4.64
C_V=5.57
THRUST
C.G. POS.
ELEV.
APPLIED MOMENT & RESISTANCE VS. TRIM ANGLE AT FIXED SPEEDS
TRIM ANGLE, DEG.

Figure 16.-